Summer 8-15-2021

Testing Candidate Cerebellar Presymptomatic Biomarkers for Autism Spectrum Disorder

Zoe Wilson Hawks
Washington University in St. Louis

WASHINGTON UNIVERSITY IN ST. LOUIS

Department of Psychological and Brain Sciences

Dissertation Examination Committee:
Lori Markson, Chair
Desirée White, Co-Chair
Richard Abrams
John Constantino
John Pruett

Testing Candidate Cerebellar Presymptomatic Biomarkers for Autism Spectrum Disorder

by
Zoë Wilson Hawks

A dissertation presented to
The Graduate School
of Washington University in
partial fulfillment of the
requirements for the degree
of Doctor of Philosophy

August 2021
St. Louis, Missouri

Table of Contents

List of Figures

List of Tables

Acknowledgments

First, I would like to thank the Infant Brain Imaging Study (IBIS) Network, who provided data for this project. IBIS is an NIH funded Autism Centers of Excellence project and consists of a consortium of universities in the U.S. and Canada. Network sites and lead investigators at the time of dissertation data acquisition and/or processing are listed below in italics.

Clinical Sites: University of North Carolina: J. Piven (Network PI), H.C. Hazlett, C. Chappell; University of Washington: S. Dager, A. Estes, D. Shaw; Washington University: K. Botteron, R. McKinstry, J. Constantino, J. Pruett; Children's Hospital of Philadelphia: R. Schultz, Juhi Pandey; S. Paterson; University of Alberta: L. Zwaigenbaum; University of Minnesota: J. Elison, J Wolff; Data Coordinating Center: Montreal Neurological Institute: A.C. Evans, D.L. Collins, G.B. Pike, V. Fonov, P. Kostopoulos, S. Das; Image Processing Core: NYU: G. Gerig; University of North Carolina: M. Styner; Statistical Analysis Core: University of North Carolina: H. Gu.

Next, I would like to thank the agencies that funded this research. This project was supported by grants from the Autism Science Foundation (19-001) and NIH (F31 MH120918, R01 HD055741, R01 MH093510, UL1 TR002345, R01 MH118362, MH118362-02S1, P50 HD103525). Computations were performed using the facilities of the Washington University Center for High Performance Computing, which were partially funded by NIH grants 1S10RR022984-01A1 and 1S10OD018091-01. Neuroimaging processing pipelines were supported by NIH grants P30NS048056 and P30NS098577.

Third, I would like to thank all the people at Washington University in St. Louis that shared their time, energy, expertise, and wisdom to make my graduate education an invigorating

period of personal and professional growth. In particular, I would like to thank my mentors for their unwavering support: Drs. Desirée White, John Pruett, John Constantino, Alexandre Todorov, and Natasha Marrus; my committee members for their valuable feedback: Drs. Lori Markson and Richard Abrams; lab mates past and present, who were consummate teammates and friends: Anna Hood, Erika Wesonga, Clarissa Tardiff, Suzin Blankenship, Tomoyuki Nishino, Muhamed Talovic, Savannah Davis, Alicia Rocca, and Rachael Wagner; and many others (collaborators, teachers, peers) who offered training and guidance throughout this process.

Fourth, I would like to thank my undergraduate research mentors at the University of Michigan, who seeded my love of psychology and provided foundational early research experiences. Thank you, Drs. Daniel Weissman and Ashley Gearhardt. (Go Blue!)

Finally, I would like to thank friends and family, who have been there to celebrate the good and cry through the bad. To my clinical cohort: Marilyn, Tasha, Kat, and E; to my STL crew: Maddy, Anna, Kendra, Shelly, Emily, and Ankita; to lifelong friends: Q, Bex, Lyss, Olivia, Sarah, Carrie, Ellen, and Izzy; to family: Kathy, Wayne, Sue, Will, Carly, Pat, Mal, and Harvey; and to those closest to it all: Mom, Dad, Matt, Austin, and Bandit. Forever grateful.

Zoë Hawks

Washington University in St. Louis

August 2021

ABSTRACT OF THE DISSERTATION

Testing candidate cerebellar presymptomatic biomarkers

for Autism Spectrum Disorder

by

Zoë Wilson Hawks

Doctor of Philosophy in Psychological and Brain Sciences

Washington University in St. Louis, 2021

Professor Lori Markson, Chair

Professor Desirée White, Co-Chair

Background: Autism spectrum disorder (ASD) is a neurodevelopmental disorder diagnosed on the basis of social impairment, restricted interests, and repetitive behaviors. Contemporary theories posit that cerebellar-mediated error signaling impairments contribute to the causation of ASD. However, the relationship between infant cerebellar functional connectivity (fcMRI) and later ASD behaviors and outcomes has not been investigated. Such work is critical to establish early (presymptomatic) cerebellar correlates of ASD. **Methods:** Data from the Infant Brain Imaging Study (*n*=94, 68 male) were used to evaluate cerebellar fcMRI as a presymptomatic biomarker for ASD. Specifically, brain-behavior associations were analyzed for 6-month cerebellar connections in relation to later (12- and 24-month) ASD behaviors and outcomes using univariate tests of association, multivariate machine learning prediction, and fcMRI enrichment. Univariate and multivariate approaches focused on cerebellar-frontoparietal network (FPN is implicated in error-signaling) and cerebellar-default mode network (DMN is implicated

in adult studies of ASD) connections, while enrichment afforded a data-driven test of whole-brain connectivity. **Results:** Univariate tests of cerebellar-FPN and cerebellar-DMN connections failed to implicate the cerebellum in ASD, despite > 80% power to detect medium-sized effects. Multivariate tests in high-risk infants using cerebellar-FPN and cerebellar-DMN connections similarly failed to achieve above-chance classification accuracy for ASD diagnosis, despite replicating procedures that achieved > 80% positive predictive value in whole-brain data. FcMRI enrichment identified correlates of ASD-associated behaviors in brain networks of a priori interest (FPN, DMN), as well as in cingulo-opercular (CO) and medial visual (mVis) networks. However, post-hoc tests did not support a unique role for cerebellar connectivity within these networks. **Conclusions:** Contrary to contemporary theories, we failed to observe a relationship between infant cerebellar fcMRI and ASD. Instead—in the first-known application of fcMRI enrichment to temporally lagged, early developmental brain-behavior associations—we identified infant control (FPN, CO), visual, and default mode correlates of later ASD behaviors. Future work may investigate whether connectivity involving these networks prospectively predicts ASD diagnosis, thereby expediting intervention and furthering etiologic understanding.

Chapter 1: Introduction

Autism spectrum disorder (ASD) is a highly heterogeneous disorder diagnosed on the basis of (1) impaired social communication and interaction and (2) restricted interests and repetitive behaviors (American Psychiatric Association, 2013). However, the defining behavioral features of ASD are not observable during the first year of life (Ozonoff et al., 2010). During this presymptomatic period, researchers have argued that infant brain abnormalities may alter sensorimotor and attentional experiences, contributing to the emergence and consolidation of ASD symptoms during the second and third years of life (Piven et al., 2017). Thus, as has been observed in neurodegenerative conditions such as Huntington's (Aylward et al., 2012) and Parkinson's (Fearnley & Lees, 1991) diseases, early brain abnormalities may represent some of the earliest-emerging signals of ASD.

1.1 Whole-brain neuroimaging data predict ASD but offer limited insights into pathophysiology

Efforts to prospectively predict individual-level ASD diagnostic outcomes highlight the shortcomings of behavioral data and, correspondingly, the importance of infant neural biomarkers. Currently, there are no first-year-of-life behavioral markers that accurately and reliably predict ASD diagnosis (Chawarska et al., 2014; Wolff & Piven, 2020). Eye-tracking biomarkers show promise (Jones & Klin, 2013), but they require repeatedly-sampled longitudinal data, and their predictive utility within high-risk samples (i.e., families with an older ASD-affected sibling) remains unclear (Wolff & Piven, 2020). High-risk infants are 12-times more likely to develop ASD compared to low risk infants (Constantino, Zhang, Frazier,

Abbacchi, & Law, 2010; Ozonoff et al., 2011). As such, accurate diagnostic prediction within high-risk samples is critical to advance clinically-actionable ASD screening.

Despite limited evidence for behaviorally-based prediction, evidence for presymptomatic prediction using neural biomarkers is accruing (Wolff & Piven, 2020). Two recent publications from IBIS (Infant Brain Imaging Study) achieved highly accurate ASD diagnostic prediction in high-risk samples using whole-brain structural (Hazlett et al., 2017) and functional connectivity (Emerson et al., 2017) magnetic resonance imaging (MRI) data. Electroencephalogram (EEG) data have also been used to develop informative predictive models of ASD (Bosl et al., 2018; Dickinson et al., 2020; Gabard-Durnam et al., 2019), although EEG has not yet demonstrated diagnostic accuracy in high-risk samples commensurate with MRI. In all instances, predictive diagnostic classifiers await successful independent replication. Replication efforts are ongoing within IBIS.

Although Emerson et al. (2017) achieved highly successful fcMRI-based ASD diagnostic prediction, their model leveraged whole-brain data (26,335 features), and features that contributed strongly to classification accuracy were distributed across the entire brain. Future specification of biologically-informed, neuroanatomically-constrained presymptomatic brain biomarkers holds potential to improve clinical and diagnostic services, while also advancing understandings of ASD etiology. In service of these goals, the present study interrogated infant cerebellar resting state functional connectivity (fcMRI) as a candidate presymptomatic biomarker of ASD using multiple analytic approaches. Support for cerebellar biomarkers would help establish specific neural correlates of ASD that are informed by behavioral theory, suggesting a relationship between early cerebellar development and later ASD diagnosis.

1.2 Findings from basic and clinical research implicate cerebellar circuitry in ASD

Bauman and Kemper first reported cerebellar atypicalities—most notably, reduced Purkinje cell count—in ASD over 35 years ago (Bauman & Kemper, 1985). In the last ten years, interest in the cerebellum among ASD researchers has risen dramatically, with some arguing that cerebellar structure and function are not simply associated with ASD but instead may play a causal role in the development of ASD (Fatemi et al., 2012; Rogers et al., 2013; Wang et al., 2014). This argument integrates findings from basic research, which have led to more refined understandings of cerebellar function and functional architecture (Buckner et al., 2011; Leggio & Molinari, 2015; Marek et al., 2018), with findings from clinical research, which suggest myriad ways in which cerebellar function may differ in individuals with ASD compared to neurotypical peers (Crippa et al., 2016; D'Mello & Stoodley, 2015). These findings are described in turn, below.

Rapidly accruing evidence from basic neuroscience provides theoretical motivation for examining cerebellar connectivity as a candidate presymptomatic biomarker in ASD. Contextualizing and extending its long-recognized role in gross motor control, recent data suggest that the cerebellum may subserve additional functions: error-signaling for adaptive movement, cognition, and social prediction (Leggio & Molinari, 2015; Peterburs & Desmond, 2016; Sokolov et al., 2017). This capability is thought to be instantiated through structural and functional cerebellar-cerebral connections (Dosenbach et al., 2006; Fiez, Petersen, Cheney, & Raichle, 1992), in which the function of a given cerebellar node is determined by its network membership. For example, a cerebellar node in the somatomotor network may subserve error-signaling for movement (Buckner, 2013; Moberget & Ivry, 2016), whereas a cerebellar node in

the frontoparietal network may subserve error-signaling following expectancy violations (Buckner, 2013; Dosenbach et al., 2007; Marek & Dosenbach, 2018). As predicted by error-signaling accounts of cerebellar function, injuries to the cerebellum and its circuitry are associated with a diverse array of sensorimotor (Marko et al., 2015), social cognitive (Hampson & Blatt, 2015; Hoche et al., 2016), and emotion regulation impairments (Schmahmann & Sherman, 1998). Heterogeneous impairments within these domains (e.g., sensory hypersensitivity, theory of mind, and heightened irritability) are observed in ASD, leading some researchers to posit that cerebellar-mediated error signaling may contribute to ASD symptomology (Freedman & Foxe, 2017; Sinha et al., 2014; Wang et al., 2014).

Evidence from fcMRI studies in children and adults further supports cerebellar theories of ASD etiology. Atypical patterns of cerebellar-cerebral connectivity have been reported among individuals with ASD (Hanaie et al., 2018; Khan et al., 2015; Oldehinkel et al., 2019; Ramos et al., 2019; Verly et al., 2014), and atypical patterns appear to persist when ASD is measured with respect to severity rather than diagnosis (Jung et al., 2014; Verly et al., 2014). In a recent comprehensive review, D'Mello & Stoodley (2015) argued that cerebellar-cerebral circuits may confer direct risk for ASD. It is worth noting, however, that the directionality of cerebellar effects (hypo- vs. hyper-connectivity) varies across studies (Crippa et al., 2016), gross cerebellar injury during adulthood rarely produces classic ASD symptoms (Manto et al., 2013; Wolf et al., 2009), and null reports (e.g., those finding no association between cerebellar connectivity and ASD severity) also appear in the literature (Carper et al., 2015; Khan et al., 2015; Padmanabhan et al., 2013). To reconcile inconsistencies, Wang et al. (2014) posited that cerebellar influences on ASD may be particularly important during early developmental "sensitive periods."

1.3 Behavioral consequences of early developmental cerebellar dysfunction are unknown

Presently, there are very few early developmental studies of the cerebellum and ASD. One structural imaging study of toddlers born prematurely observed clinically elevated scores on ASD screening checklists (Robins et al., 2001; Rutter et al., 2003) among 33-43% of participants with isolated cerebellar hemorrhagic injury (n = 35). In contrast, 0-3% of age-matched controls (n = 35) had elevated scores (Limperopoulos et al., 2007). As such, there was an approximately 36-fold increase in elevated scores on ASD screening checklists for toddlers with cerebellar hemorrhagic injury (Wang et al., 2014). In addition to these findings, a diffusion tensor imaging study (n = 217, 54 with ASD) identified prospective associations between infant cerebellar white matter pathways and later sensory responsiveness in children with ASD (Wolff et al., 2017).

Infant cerebellar fcMRI remains to be examined in relation ASD. Among studies that examined cerebellar fcMRI in older samples, cerebellar regions were frequently aggregated into a "cerebellar network," despite evidence from basic neuroscience indicating that they participate in whole-brain networks (Buckner et al., 2011; Marek et al., 2018). Given the repeated suggestion that cerebellar pathology may play a causal role in the development of ASD—and, further, given that this argument hinges on evidence for early developmental "sensitive periods" (Wang et al., 2014)—an empirical, neurobiologically-informed test of infant cerebellar contributions to ASD is long overdue.

1.4 Present study characterized the relationship between infant cerebellar-cortical functional connectivity and ASD

To this end, the present study used hypothesis- and data-driven tests to evaluate 6-month fcMRI correlates of later (12- and 24-month) ASD risk factors, symptoms, and diagnostic

outcomes (Figure 1A). Analyses were performed on previously acquired data from IBIS. Hypothesis-driven tests of univariate brain-behavior associations (Figure 1B) focused on functional connections between cerebellar and cortical regions of interest (ROIs). Cortical ROIs were located in the frontoparietal network (FPN) or default mode network (DMN). The FPN is overrepresented in the cerebellum compared to the cerebral cortex (Marek et al., 2018) and subserves error signaling in support of cerebellar error-based learning (Dosenbach et al., 2007; Dosenbach et al., 2008; Marek & Dosenbach, 2018), while the DMN is frequently implicated in adolescent and adult studies of ASD (e.g., Jung et al., 2014; Nair et al., 2020; Padmanabhan et al., 2017). Thus, our decision to examine cerebellar connectivity in relation to the FPN was motivated by theory, affording a test of cerebellar-mediated error-signaling accounts of ASD, while our decision to examine cerebellar connectivity in relation to the DMN was motivated by prior empirical literature.

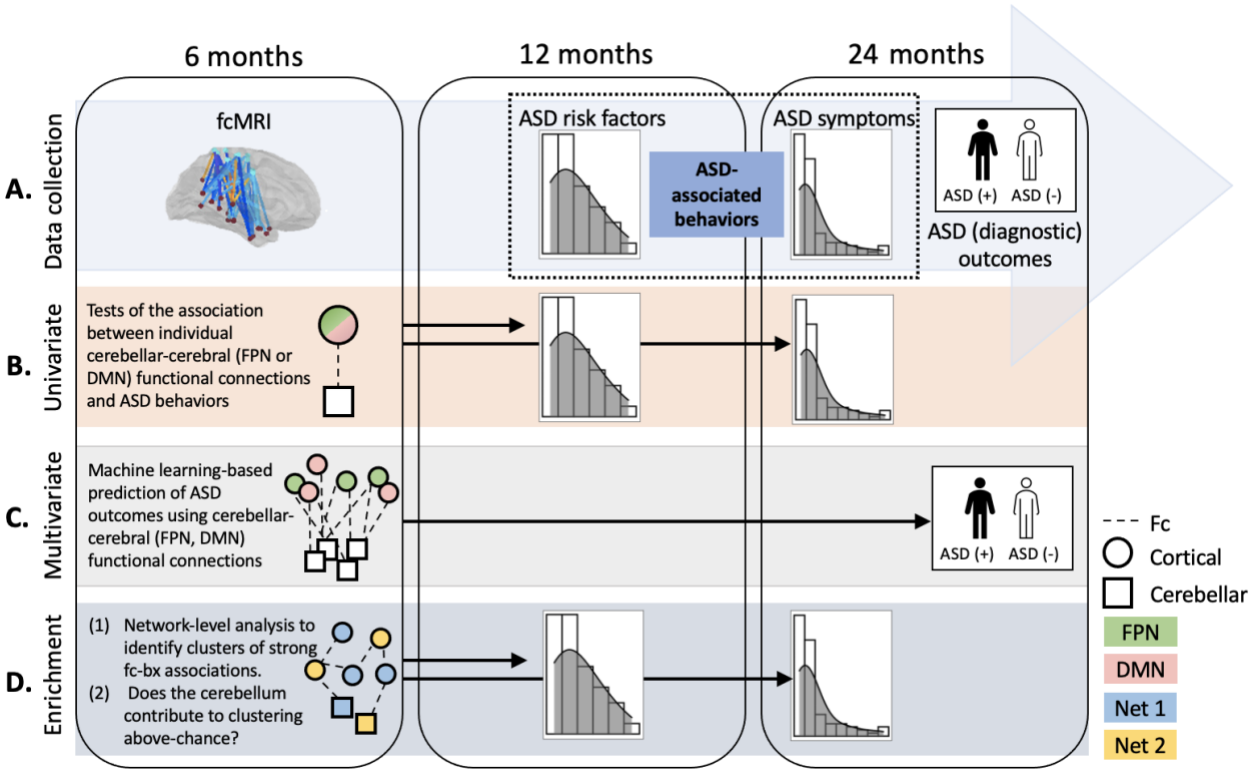

Figure 1. Study design. Summary of the (A) data collection timeline and (B-D) three-part analytic plan. Functional connectivity magnetic resonance imaging (fcMRI) data were collected at 6 months, continuous measures of ASD behavior were collected at 12 and 24 months, and ASD diagnostic outcomes were evaluated at 24 months. Circles and squares represent regions of interest (ROIs) located in the cortex and cerebellum, respectively. Colors (green, pink, blue, yellow) denote ROI network assignments (Nets 1 and 2 being arbitrary non-FPN, non-DMN networks).

Complementing univariate tests of brain-behavior associations, we used multivariate predictive classification to examine whether cerebellar connections are capable of prospectively predicting ASD diagnosis (Figure 1C). As reviewed above, prior ASD classification efforts achieved highly accurate diagnostic prediction using 6-month, whole brain fcMRI data (Emerson et al., 2017). We aimed to replicate these results using only cerebellar-FPN and cerebellar-DMN functional connections. Success therein would indicate that cerebellar information is sufficient to prospectively predict ASD diagnosis, advancing insights into ASD neurobiology.

Finally, to assess whether whole-brain cerebellar connectivity contributes to the emergence of ASD symptoms, we performed data-driven whole-brain fcMRI enrichment

analysis (Eggebrecht et al., 2017; Marrus et al., 2018; McKinnon et al., 2019) with post-hoc cerebellar randomization testing (Figure 1D). Enrichment analysis identifies clusters of strong brain-behavior associations located within and between functional brain networks, and randomization testing evaluated whether cerebellar connections contributed to clustering above-chance.

Support for cerebellar contributions to ASD would identify cerebellar functional connectivity as a promising presymptomatic biomarker of ASD, with implications for very early identification and intervention. Failure to observe significant cerebellar effects in the context of significant network enrichment results would also move the field forward, providing data-driven insights into other early underpinnings of ASD.

Chapter 2: Methods

2.1 Participants

This study involved secondary analyses of 6-month neuroimaging and 12- and 24-month behavioral data from infants who participated in IBIS at the four original network sites: University of North Carolina (UNC), Children's Hospital of Philadelphia (CHOP), Washington University School of Medicine (WUSM), and University of Washington (UW). The LORIS data management platform (Das et al., 2016) served as the behavioral, clinical, and imaging hub for this study for data collection, curation, preparation for analysis, and archiving. All families who participated in IBIS provided informed consent, approved by each site's Human Subjects Review Board. High-risk infants were defined as having at least one sibling with an ASD diagnosis. High-risk positive (HR+) infants received an ASD diagnosis (see Behavioral assessment, below) at 24-months of age, whereas high-risk negative (HR-) infants did not. Low-risk negative (LR-) infants had at least one typically developing older sibling, did not have any first or second-degree family members with ASD or intellectual disability, and did not receive an ASD diagnosis at 24-months of age. Low-risk positive (LR+) infants (n = 1) were excluded from analyses.

Genetic and family history exclusion criteria are detailed in Eggebrecht et al. (2017) and Estes et al. (2015). Briefly, participants were excluded for comorbid medical, genetic, or neurological conditions known to influence development; gestational age less than 36 weeks; birth weight less than 2000 grams; MRI contraindication; evidence of maternal substance abuse during pregnancy; or first-degree family history of major psychiatric disorder(s) such as psychosis, schizophrenia, and/or bipolar disorder.

Mann-Whitney U tests (for continuous variables) and Chi-square tests of independence (for categorical variables) were used to compare participants included in analyses to the full IBIS sample. No differences were observed with respect to behavioral scores, risk status, or diagnosis (*p*s > .05); however, the ratio of females to males was lower among participants who provided 6-month fcMRI data compared to the full IBIS sample ($p < .01$). Minor effects of site were noted for two behaviors (joint attention and fine motor functioning; *p*s = .03), driven, in both cases, by a single significant post-hoc comparison (joint attention: WUSM > UNC; fine motor functioning: UW > WUSM). There were no effects of participant sex on behavior (*p*s > .05). Participant characteristics are reported in Table 1.

Table 1. Participant characteristics. Characteristics are presented for participants with 6-month neuroimaging (fcMRI) data. *Italics* identify variables for which high scores reflect atypical behaviors; otherwise, high scores reflect typical behaviors. SD = standard deviation, BOLD = blood oxygen level dependent, CSBS-DP = Communication and Symbolic Behavior Scales Developmental Profile, IJA = initiation of joint attention, RBS-R = Repetitive Behavior Scale—Revised, MSEL = Mullen Scales of Early Learning, ADOS = Autism Diagnostic Observation Schedule, CSS = calibrated severity score, RRB = restricted interests and repetitive

	N	**%**
Sex (male)		
Male	68	72.3
Female	26	27.7
Diagnostic outcome group		
Low-risk negative	35	37.2
High-risk negative	46	48.9
High-risk positive	13	13.8
	Mean	**SD**
Age at time of scan (in months)	6.51	0.59
Number of BOLD frames (after scrubbing)	241.13	57.17
12-month behaviors		
Age at time of assessment (in months)	12.48	0.49
CSBS-DP IJA	1.44	1.38
RBS-R Restricted	0.30	0.85
RBS-R Ritualistic-Sameness	0.63	1.73
MSEL Fine Motor (T-score)	56.21	9.59
MSEL Gross Motor (T-score)	48.70	12.75
24-month behaviors		
Age at time of assessment (in months)	24.57	1.09
ADOS Total CSS	2.05	1.94
ADOS Social Affect CSS	2.39	1.98

ADOS RRB CSS	2.91	2.53

2.2 Behavioral assessment

Six-month functional connectivity was examined in relation to 12- and 24-month continuous behaviors (Figure 2) and 24-month diagnostic outcomes. Twelve-month behaviors indexed ASD risk factors, specifically: initiation of joint attention (IJA) (Dawson et al., 2004; Eggebrecht et al., 2017), fine and gross motor functioning (Marrus et al., 2018; May et al., 2016), restricted behavior (McKinnon et al., 2019), and ritualistic/sameness behavior (McKinnon et al., 2019). Twenty-four-month behaviors indexed ASD symptoms. We will refer to 12-month risk factors and 24-month symptoms collectively as "ASD behaviors" (Figure 1A), acknowledging that 12-month risk factors measure ASD-associated behaviors, whereas 24-month symptoms are definitional to ASD.

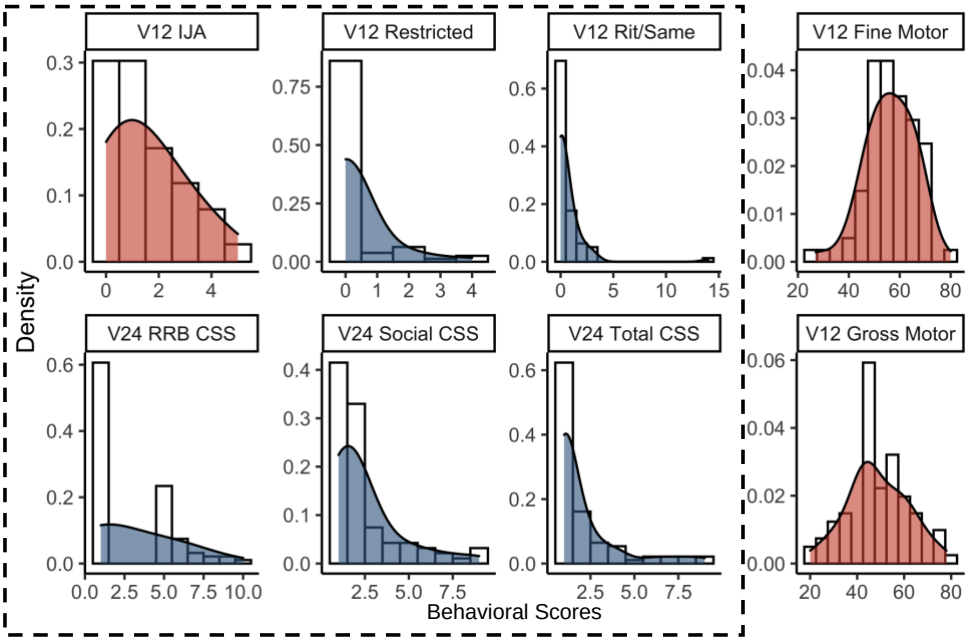

Figure 2. Distributions of behavioral scores. Combined histograms and density plots for ASD behaviors at 12- and 24-months. Left-most distributions (enclosed by dashed box) were modeled using Poisson and negative binomial regression, whereas right-most distributions were modeled using linear regression. Blue density curves

identify variables for which high scores reflect atypical behaviors; red density curves identify variables high scores reflect typical behaviors. V12 = 12-month visit, V24 = 24-month visit, IJA = initiation of joint attention, Rit/Same = ritualistic and sameness behaviors, RRB = restricted interests and repetitive behaviors. See Methods for additional details about behavioral scores (plotted along the x-axis).

Initiation of joint attention (IJA) was assessed at 12 months using the Communication and Symbolic Behavior Scales Developmental Profile (CSBS-DP) (Wetherby et al., 2002). The CSBS-DP is designed to elicit, over the course of six semi-structured sampling opportunities with an examiner, social and communicative behaviors. Consistent with Eggebrecht et al. (2017), IJA was operationalized as CSBS-DP item 7: the number of examiner-participant interactions, "used to direct another's attention to an object, event, or topic of a communicative act." (Wetherby et al., 2002). Interactions in which the child's goal was behavioral regulation were not coded as IJA.

Fine and gross motor functioning were assessed at 12 months using the Mullen Scales of Early Learning (MSEL) (Mullen, 1995). The MSEL is a standardized, clinician-administered test of developmental milestones for children 3 to 69 months of age, and it is well-validated for use in ASD (Bishop et al., 2011; Burns et al., 2013; Zwaigenbaum et al., 2005). MSEL items progress from extremely early developmental stages (e.g., "rotates head") to more advanced abilities (e.g., "walks on line"). Standardized T-scores were used in analyses.

Restricted and ritualistic/sameness behaviors were assessed at 12 months using the Repetitive Behavior Scale—Revised (RBS-R) (Bodfish et al., 2000). The RBS-R is a 43-item parent-report questionnaire validated for use in toddlers (Lam & Aman, 2007; Mirenda et al., 2010; Wolff et al., 2014). Its six subscales measure stereotyped, self-injurious, compulsive, ritualistic, sameness, and restricted behaviors. Present analyses examined counts of items endorsed rather than severity scores because prior literature suggests that counts are less

susceptible to rater bias (Wolff et al., 2014). Ritualistic and sameness subscales were combined because they load onto a common factor (Lam & Aman, 2007; Mirenda et al., 2010), and one outlier falling 7.7 standard deviations from the mean was excluded from analyses.

ASD symptom severity was assessed at 24 months using the Autism Diagnostic Observation Schedule (ADOS) (Lord et al., 2001). Continuous measures of severity were obtained by computing calibrated severity scores (CSS) across all symptoms (Gotham et al., 2009), as well as within social affect and RRB symptom domains (Hus et al., 2014). Calibrated severity scores (Gotham et al., 2009; Hus et al., 2014) were shifted to set minimum values to zero and to eliminate discontinuities (in RRB CSS) that were engendered by the scoring algorithm. As detailed in prior IBIS publications (Emerson et al., 2017; Estes et al., 2015; Hazlett et al., 2017), the ADOS (Lord et al., 2001) was used to inform clinical best estimate ASD diagnoses, which were made at 24-months by experienced clinicians who applied the Diagnostic and Statistical Manual of Mental Disorders (DSM-IV-TR; American Psychiatric Association, 2000) ASD checklist to all available testing and interview data.

2.3 Image acquisition

Data were previously collected at IBIS sites using identical, cross-site calibrated 3-T Siemens MAGNETOM TIM Trio scanners with standard 12-channel head coils. All sites followed identical protocols using gradient-echo planar image acquisition (echo time = 27 ms; repetition time = 2500 ms; voxel size 4 x 4 x 4 mm^3). Infants were naturally sleeping during scanning.

2.4 Pre- and post-processing

As in prior publications from our group (Eggebrecht et al., 2017; Emerson et al., 2017), fcMRI data were compensated for slice-dependent time shifts, head movement was quantified for spatial realignment within and across runs, whole brain image intensity was normalized to a mode value of 1,000 (Ojemann et al., 1997), and images were registered into standardized 3-mm isotropic atlas space through affine transformation. In addition, processing updates were introduced to improve image quality: atlas registration was optimized, averaged functional volumes were generated using all movement-censored frames, and calculated field map distortion correction (Gholipour et al., 2008) was implemented (https://4dfp.readthedocs.io/). Functional connectivity processing applied global signal regression, nuisance signal regression, spatial and temporal filtering, band pass filtering, and motion scrubbing at framewise displacement of 0.2 (Nielsen et al., 2019). All infants included in analyses provided a minimum of 6.25-minutes of scrubbed data.

2.5 Definition of regions of interest and functional connectivity computation

Computation of timeseries for the primary set of 230 regions of interest (ROIs; 10-mm-diameter, spherical) are described in Pruett et al. (2015), and ROI details are provided in Appendix A. In addition to the five cerebellar ROIs in the primary 230-ROI set, we generated four new cerebellar ROIs based on their connectivity profiles with functional networks relevant to present hypotheses: the FPN and DMN. Cerebellar ROIs were centered on voxels that exhibited maximal correlations with network average timeseries for the FPN or DMN, with one ROI placed for each hemisphere-network pair (left/right, FPN/DMN). Additional details about

cerebellar ROI placement are available in Appendix B. Functional connectivity matrices for the final set of 234 ROIs (original 230 ROIs + 4 new cerebellar ROIs) were calculated as Pearson correlations between pairs of ROI time-series (Figure 3A) and Fisher *r*-to-Z transformed for analyses. Each element of the resultant 234 x 234 correlation matrix represents a single functional connection.

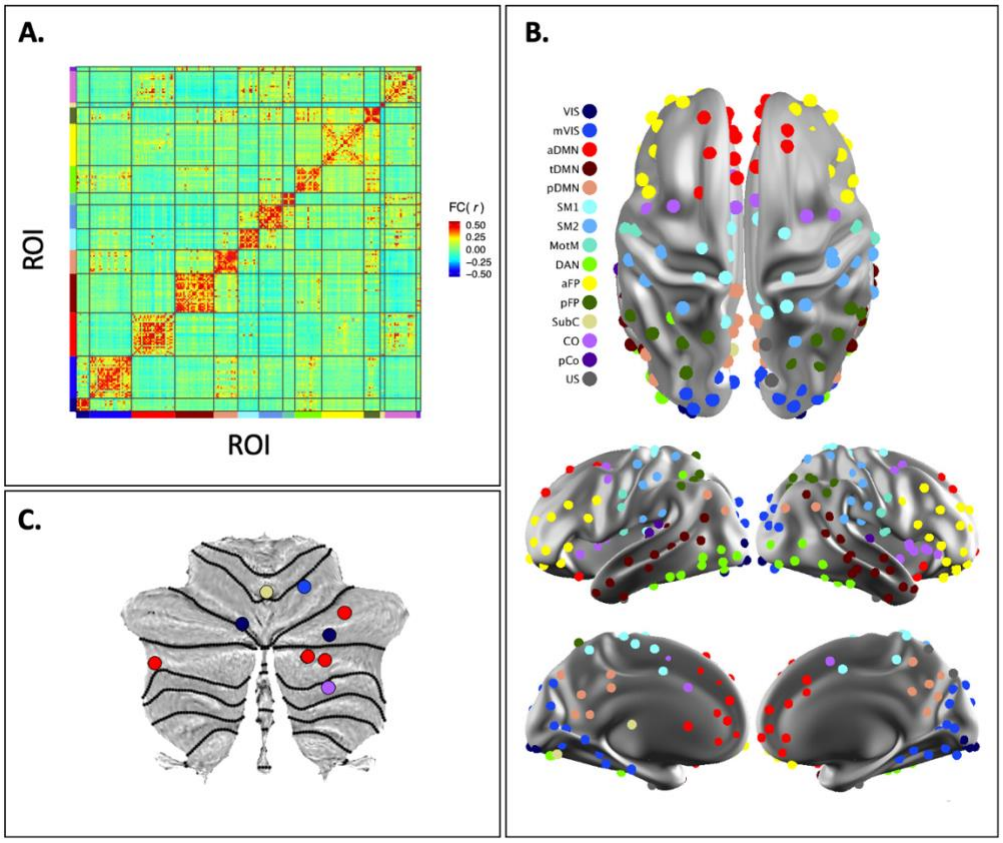

Figure 3. Functional network architecture in 6-month infants. Clockwise from top left: (A) The sample-mean fcMRI matrix depicts the correlation structure among spherical regions of interest (ROIs; n = 234). ROIs are sorted by network assignment (see legend in B), and the color gradient illustrates the strength of correlations between ROIs. Red blocks along the matrix diagonal indicate stronger correlations within, compared to between, networks. (B) Functional networks are visualized on dorsal, lateral and medial surfaces of the brain. The color of an ROI identifies its network assignment. (C) Cerebellar ROIs, also colored by network (see legend in B), are visualized on a flattened cerebellar surface (Diedrichsen & Zotow, 2015). FC(r) = functional connectivity correlation value; Vis = visual network, mVis = medial visual network, aDMN = anterior default mode network, tDMN = temporal default mode network, pDMN = posterior default mode network, SM1 = somatomotor network 1, SM2 = somatomotor network 2, MotM = motor-mouth network, DAN = dorsal attention network, aFP = anterior frontoparietal network, pFP = posterior frontoparietal network, SubC = subcortical network, CO = cingulo-opercular network, pCO = posterior cingulo-opercular network, US = unspecified/unassigned

2.6 Derivation of functional networks

To contextualize analyses, ROIs were sorted into functional brain networks using the Infomap community detection algorithm (Rosvall & Bergstrom, 2007). Infomap uses a random walk procedure to model information flow among nodes in a complex system, where paths between nodes (i.e., edges) may be binarized or weighted. The random walker will spend more time among some clusters of nodes than others, and this information is used to partition nodes into networks (Rosvall & Bergstrom, 2007). In present analyses, the sample-mean functional connectivity matrix (234 x 234) served as input to Infomap. ROIs were coded as nodes, and correlations between pairs of ROIs were coded as edges. Infomap requires a sparse matrix, so edges were thresholded at densities ranging from 2% to 10%, preserving only the strongest correlations (Appendix C). Thresholding was performed separately within structural components (cortical, subcortical, and cerebellar) rather than across the entire brain to better integrate subcortical and cerebellar ROIs into brain-wide networks (Marek et al., 2018). A weighted-voting procedure was used to identify a single, consensus network structure ("network solution") across the range of edge densities provided (Figure 3B; Seitzman et al., 2020). Network names were determined by comparing our 6-month network solution to existing toddler and adult solutions (Appendix D), balancing neuroanatomical considerations. ROIs unassigned to specific networks by Infomap (n = 4) were excluded from multivariate and enrichment analyses.

2.7 Statistical analysis

Univariate analyses were conducted in R Studio (version 3.5.1; R Core Team, 2018), and machine learning analyses were conducted in Python (version 3.8.2; Van Rossum & Drake Jr, 1995). Packages included *tidyverse* (in R; Wickham et al., 2019) and *scikit-learn* (in Python;

Pedregosa et al., 2011). Enrichment analyses were implemented in Python using in-house software.

2.7.1 Univariate associations

To evaluate whether 6-month cerebellar connectivity contributes to the development of ASD, we first tested individual cerebellar-FPN and cerebellar-DMN connections in relation to ASD risk factors and symptoms. For each subject, we isolated cerebellar connections of interest (n = 252; 9 cerebellar ROIs x 28 FPN and DMN ROIs) from the whole-brain (234 x 234) Fisher Z-transformed correlation matrix. Next, we used generalized linear models to examine univariate associations between each cerebellar connection (modeled as Fisher Z-transformed correlation values) and each ASD behavior (at 12-months: IJA, fine motor functioning, gross motor functioning, restricted behaviors, and ritualistic-sameness behaviors; at 24-months: ASD total symptom severity, social symptom severity, and RRB symptom severity).

Based on the shape of behavioral distributions (Figure 2), Poisson regression was determined to be appropriate for CSBS, RBS-R, and ADOS variables, whereas linear regression was determined to be appropriate for MSEL fine and gross motor variables. To ascertain robustness given intermittent evidence for over-dispersion (Gardner et al., 1995), we compared results from Poisson models to results from corresponding negative binomial models, looking for convergence. Empirical p-values were calculated using randomization testing (n = 5,000 reshuffles). Details about randomization testing are provided in Figure 4. To balance statistical rigor and power considerations, false-discovery rate (FDR) correction for multiple comparisons was performed with respect to the number of functional connections (n = 252) but not the

number of behaviors (n = 8). Cerebellar-cerebral functional connections were deemed significant at FDR *q*-values < 0.05.

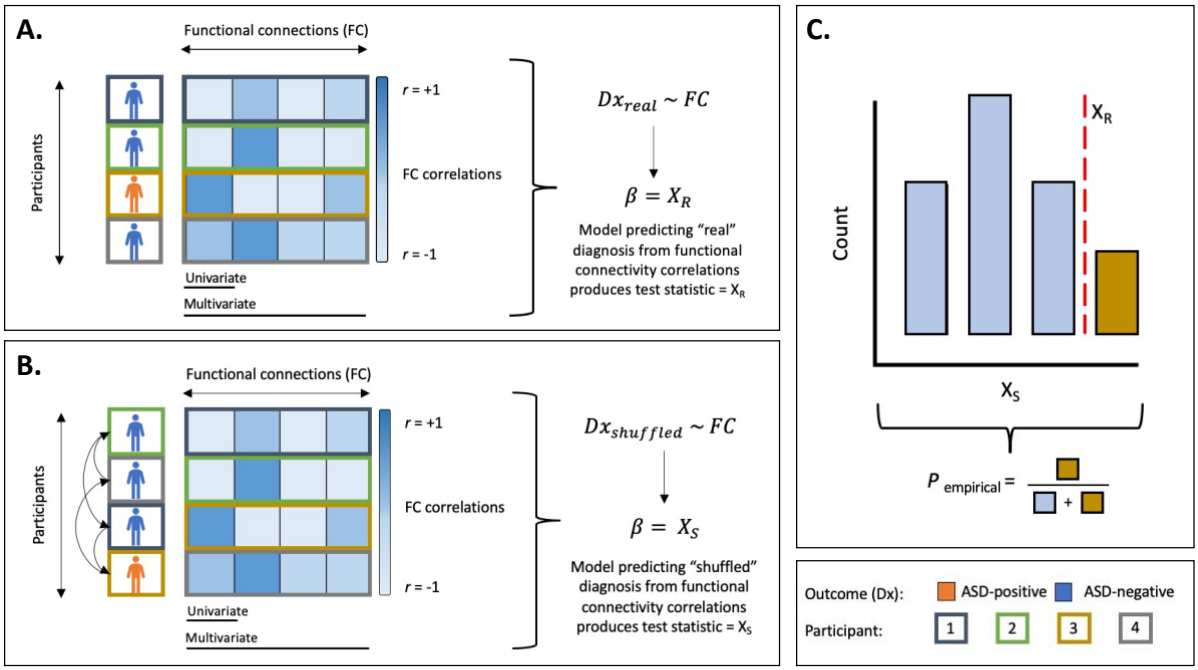

Figure 4. Randomization testing. Randomization testing is a permutation-based approach used to compute empirical *p*-values (Edgington, 2011; Knijnenburg et al., 2009). Our application of randomization testing proceeded as follows. (A) First, we computed a test statistic using experimental data (X_R). For univariate analyses, test statistics were computed using a single functional connection. For multivariate and enrichment analyses, test statistics were computed using multiple functional connections. (B) Second, we randomized behaviors or diagnostic outcomes to break the association between dependent (behavior/diagnosis) and independent (functional connectivity) variables, and we computed a test statistic using shuffled data (X_S). (C) Part B was repeated many times to build a "randomization distribution" of test statistics from shuffled data. Empirical p-values were calculated as the proportion of test statistics (X_S) in the randomization distribution that were as extreme or more extreme than the real test statistic (X_R). Dx = diagnosis; FC = functional connections; X_R = test statistic obtained in real data; X_S = test statistic(s) obtained in shuffled data; P = *p*-value

2.7.2 Multivariate machine learning prediction

Complementing univariate approaches, which are well-suited for identifying strong individual functional connections, multivariate machine learning approaches examine the collective utility of many functional connections—each of which, individually, may explain relatively little variance in the outcome of interest. Prior work from the IBIS Network achieved

highly accurate (positive and negative predictive values > 95%) diagnostic outcome prediction using whole-brain functional connections at 6-months (Emerson et al., 2017). To determine whether highly accurate 24-month diagnostic prediction is attainable using exclusively cerebellar predictors, we replicated Emerson and colleagues' (2017) approach using 6-month cerebellar-FPN and cerebellar-DMN functional connections (ROIs assigned to networks using our 6-month network solution).

Detailed methods are provided in Emerson et al. (2017). Briefly, support vector machine (SVM) learning classifiers were trained and tested in a high-risk sample (n = 59) using nested, leave-one-out cross validation (LOOCV). SVM is a supervised machine learning algorithm that solves two-group classification problems. Nested LOOCV describes an approach for training and testing machine learning classifiers to obtain unbiased estimates of performance (Figure 5).

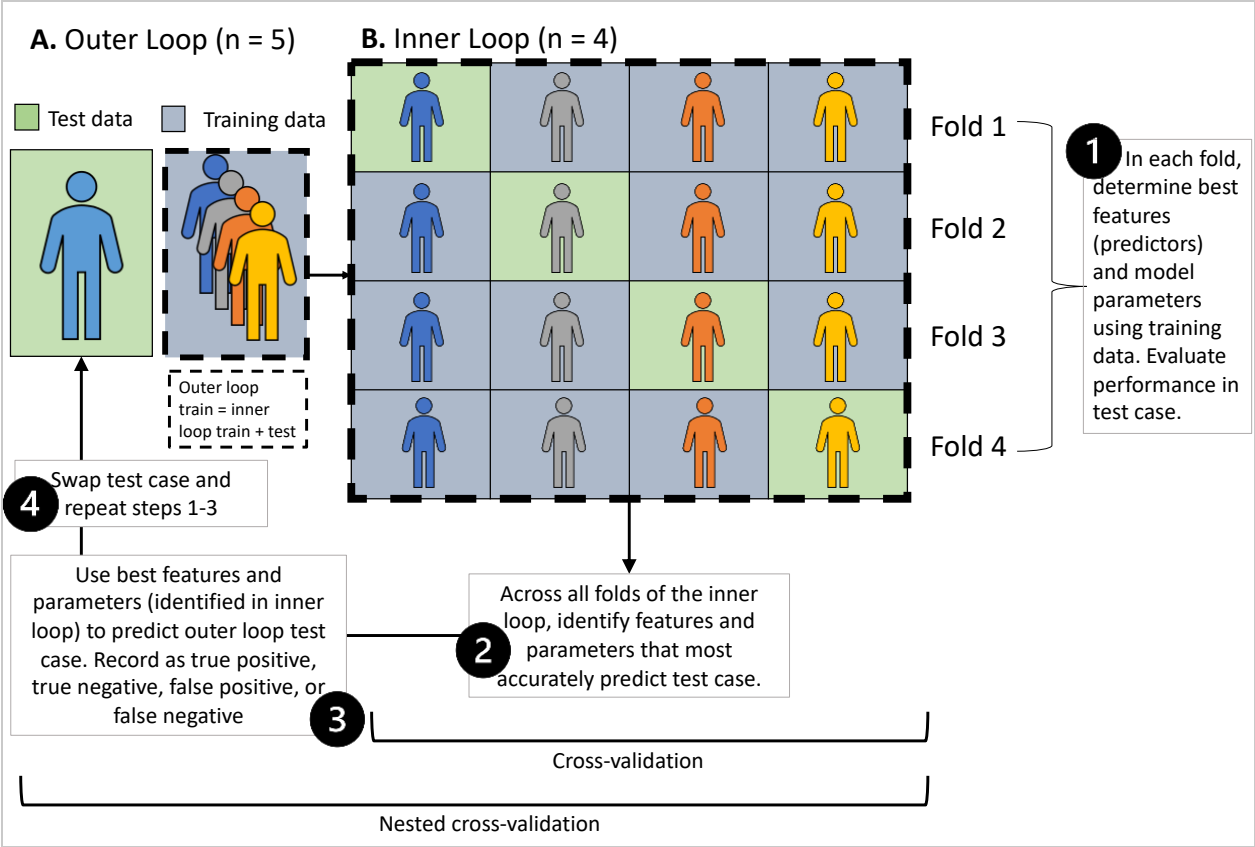

Figure 5. Leave one out cross-validation. Schematic illustrating nested, leave one out cross-validation (LOOCV) in a hypothetical sample of n = 5 participants. LOOCV is a specific instantiation of k-fold cross validation in which the number of folds k equals the number of individuals in the sample. (A) Each individual in the sample is a test case in the outer loop one time, and the remaining individuals (n = 4) are used for training the outer loop. (B) Outer loop training data are passed to the inner loop for training and testing. Each individual is a test case in the inner loop one time, and the remaining individuals (n = 3) are used for training. Feature (predictor) selection and model parameter tuning are described in steps 1-4, below. For cross validation without nesting, the entire sample undergoes the procedure described by the inner loop, and performance is averaged across folds.

We limited our sample to high-risk (HR) infants because of the present goal of differentiating positive ASD cases from negative controls in the context of shared familial liability (i.e., HR+ vs. HR-). Feature selection was based on the strength of correlations between functional connections and ASD behaviors (both 12- and 24-month). To be included as a feature in the outer cross validation loop, we required that a functional connection exhibit at last one nominally significant behavioral correlation (at $p < .05$) across all folds of the inner cross validation loop. Hyperparameter tuning was conducted in the inner cross validation loop over a

range of regularization values (C: [0.001, 10.0]) using a linear kernel (Emerson et al., 2017). Regularization values determine the penalty for misclassification (larger values = higher penalties), and kernels determines the shape of the decision function (which is the basis for prediction). To account for class imbalance (~3*x* as many HR- as HR+ infants), regularization values were weighted to be inversely proportion to class frequencies, thereby imposing a stronger misclassification penalty on minority (HR+) cases (Emerson et al., 2017; Pedregosa et al., 2011).

2.7.3 fcMRI enrichment

Whole-brain, data-driven fcMRI enrichment approaches identify functional brain network pairs that contain clusters of strong brain-behavior associations (Eggebrecht et al., 2017; Marrus et al., 2018; McKinnon et al., 2019). To assess whether cerebellar contributions to ASD behaviors are detectable in a larger search space, including but not limited to cerebellar connections with the FPN and DMN, we first identified network pairs that contained dense clusters of strong brain-behavior associations. These network pairs were said to be "enriched" for brain-behavior associations. We then performed post-hoc testing to quantify the extent to which cerebellar connections were overrepresented in enriched networks.

Our approach proceeded in three steps, improving upon prior IBIS publications (Eggebrecht et al., 2017; Marrus et al., 2018; McKinnon et al., 2019) by accounting for familywise error rate with respect to the number of network pairs tested. First, the strongest 5% of brain-behavior associations (hereafter, *hits*) were identified in real and shuffled (n = 50,000) data using mass univariate screening (Poisson or linear regression, as described above). Second, for every within- and between-network pair, empirical p-values were computed as the fraction of

shuffled runs with at least as many hits as real data (Figure 4). Based on simulations, it was determined that *p*-values < .001 were necessary to approximate a 5% false-positive rate. To avoid overlooking potentially informative results, *p*-values < .01 were also considered significant if they demonstrated the capacity to significantly predict behavior in secondary validation (see below).

2.7.4 Secondary enrichment validation

Secondary validation analyses were conducted to verify that brain information from enriched ($p < .01$) networks could be leveraged to predict behaviors relevant to ASD. Though circular (enrichment identified networks based on behavior; enrichment-derived networks were used to predict behavior), this approach nonetheless provided an important test of multimethod convergence to corroborate the behavioral significance of enriched networks. Generalized linear models (poisson or linear regression, as indicated by distributions; see Methods) were used to predict behaviors, with principal component analysis (PCA) for feature reduction. Principal component analysis is a dimensionality reduction technique that summarizes data by projecting it onto a small number of vectors ("principal components") (Ringnér, 2008).

Feature reduction (*n* components: [1, 10]), hyperparameter tuning of regularization parameters (Poisson *alpha*: [0.0001, 3.2], logistic *C*: [0.0001, 10.0]), training, and testing were performed within five-fold cross-validation. Five-fold cross-validation proceeds by partitioning a sample into five, approximately equal-sized subgroups. Each subgroup serves as a test dataset one time, and remaining data are used for training (refer to Figure 5B for an illustration of cross-validation). Prediction errors were averaged across test sets, providing an unbiased estimate of

performance, and empirical *p*-values were computed by comparing the mean prediction error in real and randomized data over $n = 500$ runs (Figure 4).

2.7.5 Post-hoc randomization

Post-hoc randomization testing (n = 10,000 reshuffles) examined whether cerebellar ROIs were overrepresented among the 5% strongest brain-behavior associations (*hits*) within a significantly enriched network pair. To this end, continuous behaviors were shuffled with respect to functional connections (Figure 4). Cerebellar involvement was quantified as the number of hits (nC) that included at least one cerebellar ROI. Empirical *p*-values were computed as the fraction of the randomization distribution in which $n\text{C}_{\text{random}} > n\text{C}_{\text{real}}$. Significant coaggregation of cerebellar-cerebral functional connections in the top 5% of the randomization distribution would identify important cerebellar contributions to ASD, affording a whole-brain, data-driven counterpart to hypothesis-driven tests of the FPN and DMN.

Chapter 3: Results

3.1 Univariate associations

Hypothesis-driven tests evaluating individual associations between 6-month cerebellar-FPN and cerebellar-DMN functional connections (n = 252) and later ASD behaviors (at 12-months: IJA, fine motor functioning, gross motor functioning, restricted behaviors, and ritualistic-sameness behaviors; at 24-months: ASD total symptom severity, social symptom severity, and RRB symptom severity) failed to implicate the cerebellum in ASD (Figure 6) despite adequate statistical power to detect medium-sized effects (Figure 7). Prior to FDR correction, 5.6% of univariate tests were significant at $p < .05$ (as would be expected by chance). Following FDR correction, no significant results remained at $q < .05$.

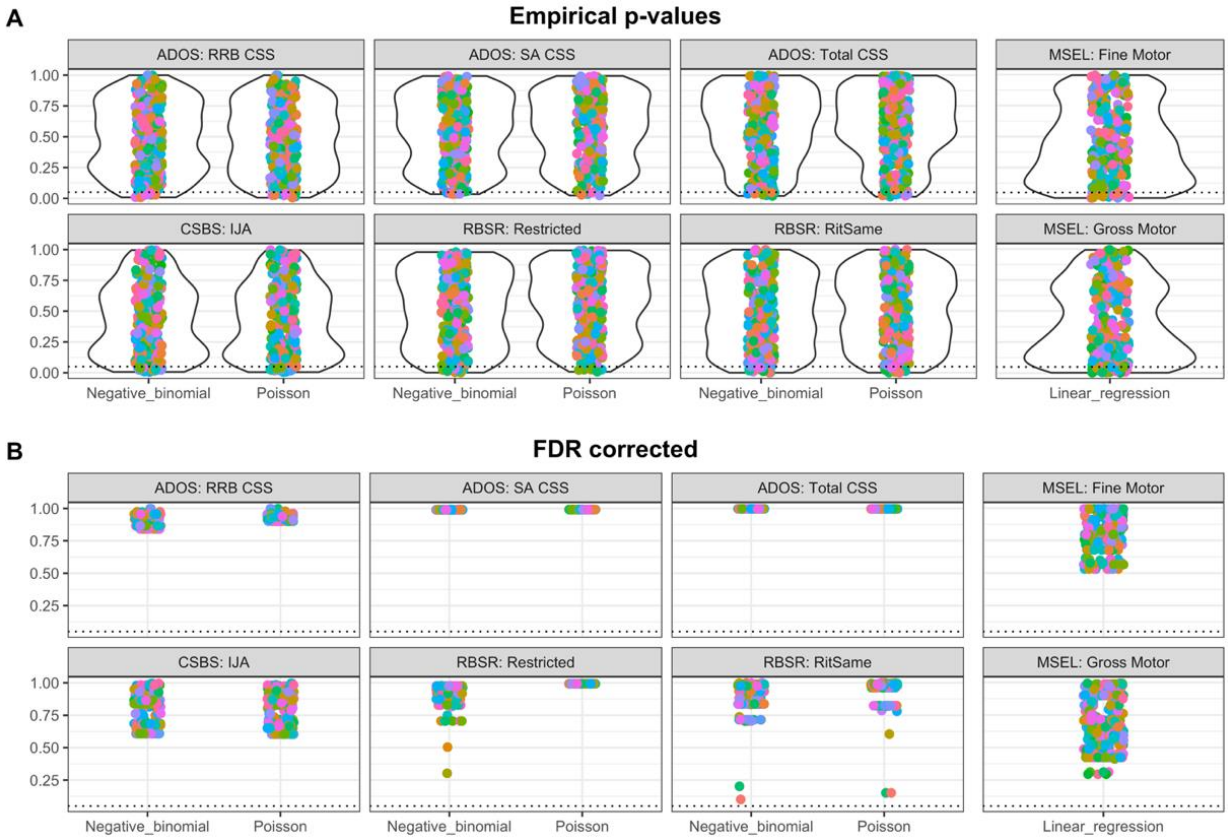

Figure 6. Univariate tests of cerebellar connections. Hypothesis-driven tests of brain-behavior associations between cerebellar-FPN and cerebellar-DMN connections (n = 252) and ASD behaviors (n = 8). Each dot visualizes the results from a single Poisson, negative binomial, or linear regression model (plotted on x-axis), with (A) empirical p-values and (B) FDR-corrected q-values plotted on the y-axis. Colors aid discrimination of dots, and vertically-oriented kernel density plots (in A) illustrate the distribution of dots across the range of p-values (n = 252 per violin). The threshold for significance (p, q < .05) is indicated by a dotted black line. After FDR correction, no significant results remained at q < .05. The smallest FDR-adjusted q-value was obtained for a cerebellar-cerebral connection between two anterior default mode ROIs in relation to 12-month ritualistic-sameness behavior (negative binomial: *beta* = -4.49, SE = 1.27, q = 0.10; Poisson: *beta* = -3.98, SE = 1.01, q = 0.15). FDR = false discovery rate, SE = standard error, CSBS = Communication and Symbolic Behavior Scales, IJA = initiation of joint attention, ADOS = Autism Diagnostic Observation Schedule, CSS = calibrated severity score, RRB = restricted interests and repetitive behaviors, SA = social affect, RBS-R = Repetitive Behavior Scale—Revised, RitSame = ritualistic and sameness, MSEL = Mullen Scales of Early Learning

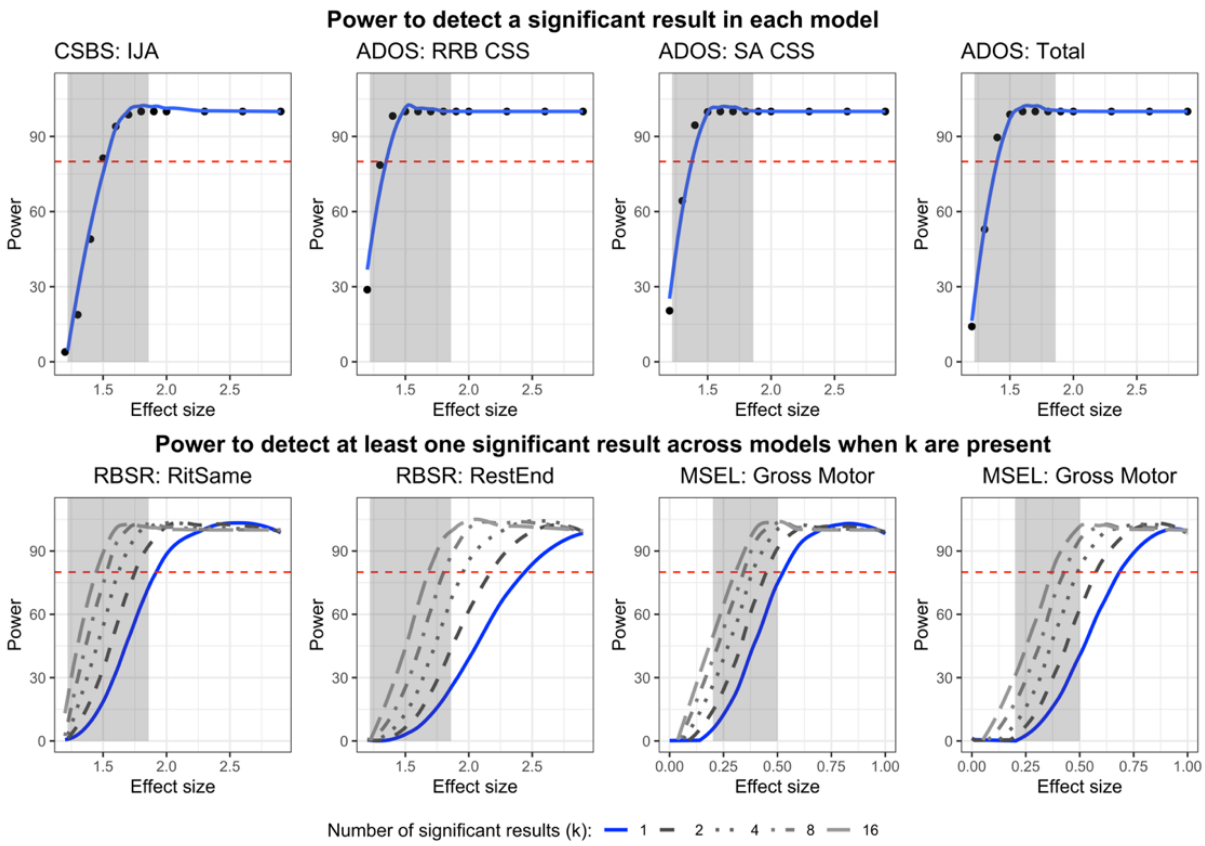

Figure 7. Statistical power. Power was calculated in R (simr package) using Monte Carlo simulation for Poisson and linear regression (Green & Macleod, 2016; R Core Team, 2018), with Bonferroni correction to account for the number of functional connections per behavior. Effect sizes for Poisson regression (CSBS, RBSR, ADOS) were estimated as incidence rate ratios (IRR), where 1.22, 1.86, and 3.00 represent small, medium, and large effects, respectively (Olivier et al., 2017). Effect sizes for linear regression (MSEL) were estimated using Cohen's conventions, where 0.2, 0.5, and 0.8 represent small, medium, and large effects, respectively (Cohen, 1988). Small-to-medium sized effects are shaded in gray. For CSBS and ADOS variables (top), we were well-powered (80%, indicated by red line) to detect medium effects in individual models. For RBS-R and MSEL variables (bottom), we were well-powered to detect at least one significant medium effect assuming multiple significant medium effects were present across models, as would be expected if the cerebellum were a major driver of ASD behaviors in early development. CSBS = Communication and Symbolic Behavior Scales, IJA = initiation of joint attention, ADOS = Autism Diagnostic Observation Schedule, CSS = calibrated severity score, RRB = restricted interests and repetitive behaviors, SA = social affect, RBS-R = Repetitive Behavior Scale—Revised, MSEL = Mullen Scales of Early Learning

3.2 Multivariate machine learning prediction

Multivariate machine learning analyses (SVM with nested, leave one out cross-validation) aimed to predict ASD diagnosis (i.e., HR+ vs. HR-) using cerebellar-FPN and cerebellar-DMN functional connections. In the context of familial risk (~1/5 chance of developing ASD), a machine that exclusively predicts the minority class (HR+) will achieve ~20% positive predictive value (PPV), providing a baseline for classifier performance evaluation. Our classifier failed to significantly exceed 20% PPV (observed PPV = 23%), and performance was similarly poor with respect to other metrics (accuracy = 66%, sensitivity = 23%, specificity = 78%, NPV = 78%), indicating that cerebellar-FPN and cerebellar-DMN features are insufficient to inform diagnostic outcome prediction (cf. Emerson et al., 2017, who applied identical methods to whole-brain data and obtained accuracy = 97%, sensitivity = 82%, specificity = 100%, PPV = 100%, and NPV = 96%).

3.3 fcMRI enrichment

Data-driven, whole-brain fcMRI enrichment identified four 6-month network pairs that exhibited strong associations with later ASD behaviors (Figure 8A). In relation to 12-month RBS-R restricted behaviors, clustering of brain-behavior associations was observed between somatomotor network 1 (SM1) and the temporal default mode network (tDMN; $p < .006$). In relation to 24-month ADOS RRBs, clustering of brain-behavior associations was observed between the posterior frontoparietal network (pFP) and the medial visual network (mVis; $p < .006$). In relation to 12-month MSEL fine motor functioning, clustering of brain-behavior associations was observed between the anterior frontoparietal network (aFP) and the posterior default mode network (pDMN; $p < .010$). Finally, in relation to 12-month MSEL gross motor

functioning, clustering of brain-behavior associations was observed between the cingulo-opercular network (CO) and the anterior default mode network (aDMN; $p < .007$). Network enrichment was not observed for 12-month IJA, 12-month ritualistic-sameness behavior, 24-month ASD total symptom severity, nor 24-month ASD social symptom severity.

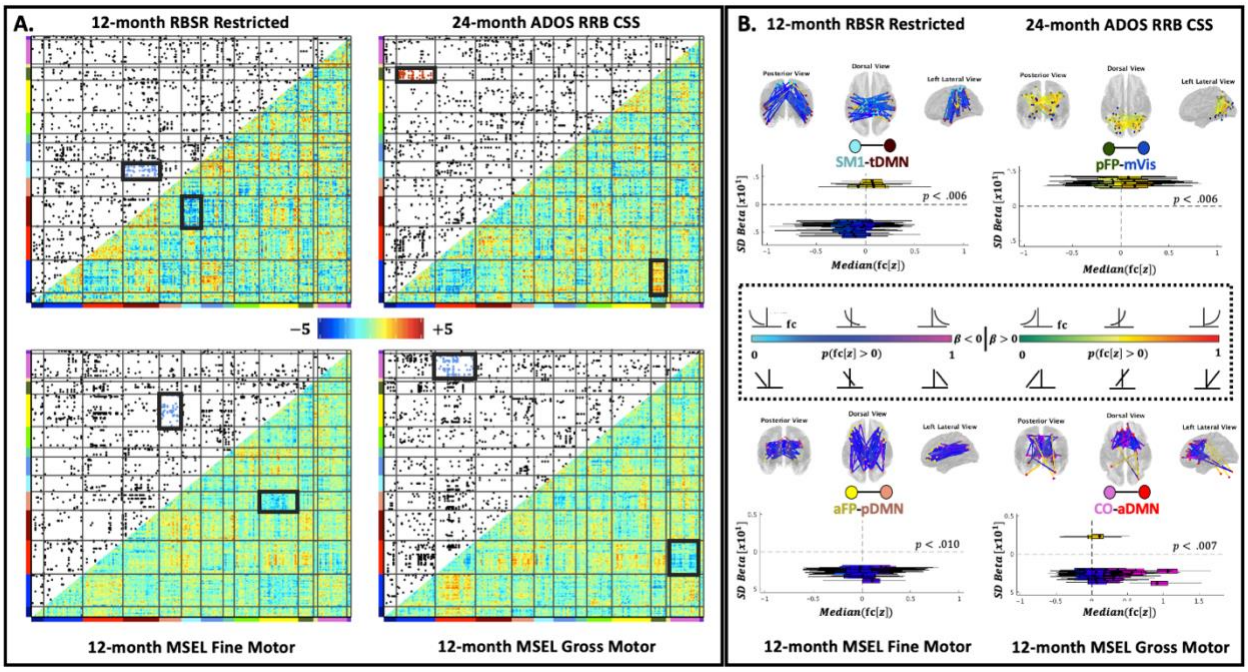

Figure 8. fcMRI enrichment. (A) Within and between networks, clusters of brain-behavior associations were identified using enrichment. Lower triangles depict standardized beta coefficients. Upper triangles were generated by applying a 5% threshold to standardized beta coefficients. Each black dot represents a single, strong brain-behavior association. (B) Six-month functional connections between SM1-tDMN, pFP-mVis, aFP-pDMN, and CO-aDMN were strongly associated with 12- and 24-month motor functioning and RRBs. Within enriched network pairs, locations of strong brain-behavior associations are visualized on posterior, dorsal, and lateral views of the brain (top). Box plots (bottom) further illustrate the range of functional connectivity values in the study sample (x-axis) that underlie each brain-behavior correlation (y-axis). Blue-pink and green-red color gradients identify negative and positive brain-behavior associations, respectively. Specific colors denote the sign and strength of functional connectivity (e.g., pale blue/green = predominantly negative connectivity; pink/red = predominantly positive connectivity). All network pairs except SM1-tDMN passed our secondary validation protocol.

3.4 Secondary enrichment validation

All four enriched ($0.001 < p < 0.01$) network pairs were subjected to secondary validation (i.e., cross-validated prediction of ASD behaviors using enriched networks). Three of four 6-month network pairs passed secondary validation (Appendix E). These included: pFP-mVis (p =

0.04), aFP-pDMN (p = 0.03), and CO-aDMN (p = 0.01). Between pFP and mVis, increased positive functional connectivity was associated with increased 24-month RRBs (Figure 8B). Between aFP and pDMN, increased positive functional connectivity was associated with decreased 12-month fine motor functioning. Finally, between CO and aDMN, increased positive functional connectivity was associated with decreased 12-month gross motor functioning. SM1-tDMN did not pass secondary validation (p = 0.15) and will not be interpreted further.

3.5 Post-hoc randomization

Two of three network pairs that passed secondary validation also contained cerebellar ROIs: CO-aDMN and pFP-mVis. Significant aggregation of cerebellar functional connections was not observed among hits in either network pair (ps = 0.08 and 0.49 for CO-aDMN and pFP-mVis, respectively) (Appendix F).

Chapter 4: Discussion

Contrary to contemporary hypotheses, we failed to observe a relationship between 6-month cerebellar fcMRI and later ASD behaviors and outcomes. Univariate tests of cerebellar-FPN and cerebellar-DMN connections were not associated with 12- or 24-month ASD behaviors, despite adequate statistical power (> 80%) to detect medium-sized effects. In addition, multivariate tests of cerebellar-FPN and cerebellar-DMN connections did not achieve above-chance ASD diagnostic classification accuracy, despite replicating procedures that achieved > 90% PPV in brain-wide work (cf. Emerson et al., 2017). Although data-driven fcMRI enrichment identified multiple infant network correlates for later ASD behaviors, post-hoc randomization tests did not support a unique role for infant cerebellar connectivity within enriched network pairs. Together, these results cast doubt on cerebellar theories of ASD etiology, indicating that cerebellar connectivity effects, if present, are likely small. Instead, cerebellar participation in network enrichment may contribute to the emergence of ASD behaviors in the broad context of non-cerebellar functional connections.

4.1 fcMRI enrichment analysis identified network correlates of ASD behaviors

Although cerebellar functional connections failed to predict ASD behaviors and outcomes, the present fcMRI enrichment results nonetheless suggest a path forward for research. Using enrichment, we identified three clusters of brain-behavior relationships involving infant frontoparietal, cingulo-opercular, and default mode networks (FPN, CO, and DMN, respectively). Specifically, enrichment was observed between: (1) pFP and mVis, in which more positive connectivity preceded increased 24-month RRBs; (2) aFP and pDMN, in which more

positive connectivity preceded poorer 12-month fine motor functioning; and (3) CO and aDMN, in which more positive connectivity preceded poorer 12-month gross motor functioning.

This pattern of results reinforces our decision to focus hypothesis-driven tests on FPN (implicated in error-signaling; Dosenbach et al., 2007; Marek & Dosenbach, 2018) and DMN (commonly implicated in ASD; e.g., Jung et al., 2014; Nair et al., 2020; Padmanabhan et al., 2017) connections. Although we did not make a priori hypotheses about the cingulo-opercular (CO) network, the CO (much like the FPN) subserves error-signaling in support of error-based learning (Dosenbach et al., 2008; Neta et al., 2014; Power & Petersen, 2013). Thus, FPN and CO representation within enriched network pairs raises the possibility that ASD behaviors may reflect cortically-mediated error-signaling impairments. Behavioral studies are necessary to directly test this hypothesis.

DMN representation within enriched network pairs, meanwhile, supports the downward extension of findings from older individuals, which have commonly implicated the DMN in ASD (e.g., Jung et al., 2014; Nair et al., 2020; Padmanabhan et al., 2017). Despite being consistently implicated in ASD, patterns of DMN results (e.g., hypo- vs. hyper-connectivity) vary across studies (Abbott et al., 2016; Chen et al., 2017; Duan et al., 2017; Guo et al., 2019; Nair et al., 2020). To account for this variation, it may be important to consider potential moderating effects of age. Indeed, a recent study by Lawrence et al. (2019) found that DMN-control network connectivity differed between individuals with ASD and typically developing individuals during late, but not early, adolescence. Accruing evidence (summarized below) suggests that characterizing trajectories of within- and between-DMN connectivity even earlier

in development (e.g., during infancy, as in the present study) may be fundamental to advancing understanding and assessment of presymptomatic risk for ASD.

4.2 Early developmental connectivity between control, sensory, and default mode systems is altered in ASD

We observed that more positive connectivity involving control (pFP, aFP, CO), default mode (pDMN, aDMN), and sensory (mVis) systems was reliably associated with atypical behaviors. To contextualize this observation, we reviewed all prior enrichment studies that examined functional connectivity in relation to ASD behaviors (Eggebrecht et al., 2017; Marrus et al., 2018; McKinnon et al., 2019; Wheelock et al., 2018). Results involving control, default mode, and sensory systems are summarized in Figure 9. Consistent with present results, more positive functional connectivity between default mode and control systems was associated with atypical behaviors. Increased connectivity between default mode and control systems has been reported in multiple psychiatric and neurodevelopmental disorders (Menon, 2018), including ASD (Mash et al., 2019), and may reflect compensatory activation (i.e., recruitment of multiple brain networks for processes typically performed by a single network; Grady et al., 2016; Park & Reuter-Lorenz, 2009) or reduced network segregation (de-differentiation; Keown et al., 2017).

Bx	Dir.	Fc-bx	Networks	Age	Reference	Key
IJA	↑	(+)	pDMN-Vis	12M	Eggebrecht et al.	A
Gross Motor	↑	(+)	tDMN-SMN	12M	Marrus et al.	A
Gross Motor	↑	(+)	aDMN-SMN	12M	Marrus et al.	A
Gross Motor	↑	(+/-)	pDMN-SMN	24M	Marrus et al.	A
Walking	↑	(+)	tDMN-SMN	12M	Marrus et al.	A
Walking	↑	(+)	tDMN-SMN2	12M	Marrus et al.	A
RitSame	↓	(-)	tDMN-Vis	12M	McKinnon et al.	A
Stereotyped	↓	(-)	tDMN-Vis	12M	McKinnon et al.	A
Fine	↑	(-)	aDMN-CO	6M FC	Present results	B
Gross Motor	↑	(-)	pDMN-aFP	6M FC	Present results	B
Gross Motor	↑	(-)	pDMN-pFP	24M	Marrus et al.	B
Walking	↑	(-)	pDMN-pFP	24M	Marrus et al.	B
Restricted	↓	(+)	tDMN-pFP	24M	McKinnon et al.	B
Stereotyped	↓	(+)	tDMN-pFP	24M	McKinnon et al.	B
RRB	↓	(+)	pFP-mVis	6M FC	Present results	C
RitSame	↓	(-)	pFP-Vis	12-24M	McKinnon et al.	C
Aiming-catching	↑	(-)	Sal-Motor	12Y	Wheelock et al.	C
Gross Motor	↑	(-)	tDMN-tDMN	12M	Marrus et al.	D
Walking	↑	(-)	tDMN-tDMN	12M	Marrus et al.	D
Balance	↑	(+)	DMN-DMN	12Y	Wheelock et al.	D
Motor (general)	↑	(+)	FP-FP	12Y	Wheelock et al.	E
Gross Motor	↑	(-)	SMN-SMN2	12M	Marrus et al.	F
Gross Motor	↑	(+)	SMN2-SMN2	12M	Marrus et al.	F
Walking	↑	(+)	SMN2-SMN2	12M	Marrus et al.	F

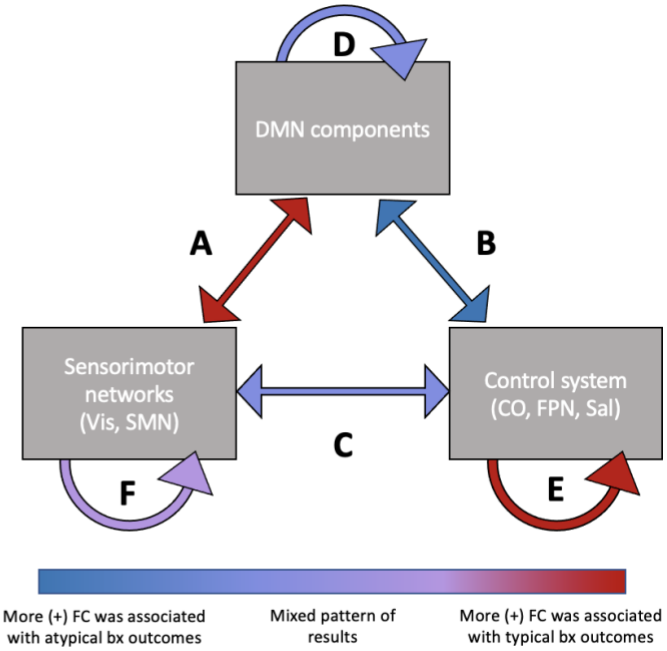

Figure 9. Empirical context. Summary of primary results* from fcMRI enrichment studies examining functional connectivity (fc) among control, DMN, and sensorimotor systems in relation to ASD behaviors (Eggebrecht et al., 2017; Marrus et al., 2018; McKinnon et al., 2019; Wheelock et al., 2018). Between networks: (A) Between sensorimotor and DMN systems, more positive fc was associated with typical behavior. (B) Between DMN and control systems, more positive fc was associated with atypical behavior. (C) Between control and sensorimotor systems, the relationship between fc and behavior was variable. Within networks: (D) Within the default mode system, the relationship between fc and behavior was variable. (E) Within the control system, more positive fc was associated with typical behavior. (F) With the sensorimotor system, the relationship between fc and behavior was variable. Fc = functional connectivity, Bx = behavior, Dir. = higher (↑) vs. lower (↓) scores reflect typical behaviors; Fc-bx = sign (positive, negative, mixed) of brain-behavior association; DMN = default mode network, Vis = visual network, SMN = somatomotor network, CO = cingulo-opercular network, FPN = frontoparietal network, Sal = salience network; M = months, Y = years. *Primary results were defined as described in primary sources. Eggebrecht et al., 2017, Marrus et al., 2018, and McKinnon et al., 2019: network pairs were significantly enriched at both ages (12 and 24 months) or were significantly enriched at one age and significantly different between ages. Present study: network pairs passed secondary validation testing

Whereas brain-behavior associations between default mode and control systems were highly consistent across studies, brain-behavior associations between sensorimotor (e.g., Vis, mVis) and control systems were variable (Figure 9C). This may be due to the fact that enrichment studies sampled brain and behavior across multiple stages of development. During early development, visual brain circuitry is argued to influence experience-dependent learning,

contributing (in some individuals) to the emergence of the ASD phenotype during the second year of life (Piven et al., 2017). At the same time, aspects of the control system are posited to flexibly modulate input from other brain systems, scaffolding age-appropriate learning and behavior (Werchan & Amso, 2017). Thus, connectivity between visual and control systems during infancy may support the acquisition of behaviors that are commonly impaired in ASD, including visual attention, language, and cognitive flexibility (Rosen et al., 2019). Similar interactions between visual and control systems during early childhood may have different behavioral sequelae. Together with results implicating the DMN in ASD during infancy, these results suggest that characterizing early developmental changes between control (FPN, CO), default mode, and sensorimotor systems may substantively advance understandings of when, where, and how brain connectivity relates to the emergence of atypical behaviors in ASD.

4.3 Limitations

The present work represents, to the best of our knowledge, the largest analysis of cerebellar functional connectivity in a prospective infant sample at risk for ASD. There were, however, a number of limitations. First, although simulation-based power analyses suggested sufficient power to detect medium-sized brain-behavior effects (Green & Macleod, 2016), identifying small-sized, reproducible effects may require even greater statistical power (Marek et al., 2020). Second, we analyzed data from nine cerebellar ROIs, and it is unclear whether results generalize to other regions in the cerebellum. We optimized cerebellar ROI placement to test hypotheses about the FPN and DMN, and future studies might instead optimize cerebellar ROI placement to test hypotheses about sensorimotor networks. Third, our measures of autism severity were developed in individuals with ASD (Gotham et al., 2009) and exhibited limited

variability in the study sample, possibly attenuating brain-behavior associations. To mitigate this limitation, we used modeling techniques well-suited for skewed data. Finally, cerebellar contributions to ASD may be more evident during different developmental epochs (e.g., prior to 6 months) or using different imaging modalities (such as diffusion tensor imaging) (Wolff et al., 2017), cautioning against over-interpretation of null results.

4.4 Future directions

Despite limitations, the present study provides an important set of results to counter strong statements that have been made about cerebellar dysfunction as a causal influence on ASD during early development (D'Mello & Stoodley, 2015; Fatemi et al., 2012; Wang et al., 2014). We suggest that future research focused on the infant cerebellum should: recruit larger samples to enhance statistical power to detect subtle effects; densely sample multiple timepoints during the first few years of life to facilitate identification of developmental epochs that may be acutely sensitive to cerebellar disturbance (Wang et al., 2014); and examine cerebellar structure and function in tandem. Although post-hoc randomization testing did not support a unique role for infant cerebellar connectivity, it remains possible that the cerebellum may influence ASD behaviors in the broad context of enriched networks (that include cerebellar and non-cerebellar connections). A promising direction for future studies may be to investigate whether 6-month connectivity between enriched network pairs (aFP-pDMN, CO-aDMN, pFP-mVis) can be used to identify infants at elevated risk for atypical development, thereby expediting early intervention (Shen & Piven, 2017).

4.5 Conclusions

The present study examined infant cerebellar connectivity as a presymptomatic neural biomarker of ASD using multiple analytic approaches. Contrary to hypotheses, we failed to observe strong associations between 6-month cerebellar fcMRI and later ASD behaviors and outcomes. Instead, fcMRI enrichment analysis identified clusters of brain-behavior relationships between networks implicated in error-signaling (FPN and CO; Dosenbach et al., 2007) and in ASD (DMN; Nair et al., 2020). These findings provide an alternative (non-cerebellar) account for error-based learning impairments in ASD (Sinha et al., 2014; Wang et al., 2014) and support the developmental extension of adult DMN findings (e.g., Jung et al., 2014; Nair et al., 2020; Padmanabhan et al., 2017). Future work is necessary to characterize patterns of infant connectivity between the FPN, CO, and DMN in relation to potential behavioral precursors (e.g., error-based learning, motor functioning, joint attention) of second-year-of-life ASD symptoms. Such efforts hold promise to improve presymptomatic detection and intervention in ASD.

References

Abbott, A. E., Nair, A., Keown, C. L., Datko, M., Jahedi, A., Fishman, I., & Müller, R.-A. (2016). Patterns of Atypical Functional Connectivity and Behavioral Links in Autism Differ Between Default, Salience, and Executive Networks. *Cerebral Cortex (New York, N.Y. : 1991)*, *26*(10), 4034–4045. https://doi.org/10.1093/cercor/bhv191

American Psychiatric Association. (2000). *Diagnostic and statistical manual of mental disorders: DSM-IV-TR* (4th ed.).

American Psychiatric Association. (2013). Diagnostic and Statistical Manual of Mental Disorders. In *Arlington*. https://doi.org/10.1176/appi.books.9780890425596.744053

Aylward, E. H., Liu, D., Nopoulos, P. C., Ross, C. A., Pierson, R. K., Mills, J. A., Long, J. D., & Paulsen, J. S. (2012). Striatal volume contributes to the prediction of onset of Huntington disease in incident cases. *Biological Psychiatry*, *71*(9), 822–828. https://doi.org/10.1016/j.biopsych.2011.07.030

Bauman, M., & Kemper, T. L. (1985). Histoanatomic observations of the brain in early infantile autism. *Neurology*, *35*(6), 866–874. https://doi.org/10.1212/WNL.35.6.866

Bishop, S. L., Guthrie, W., Coffing, M., & Lord, C. (2011). Convergent validity of the Mullen Scales of Early Learning and the Differential Ability Scales in children with autism spectrum disorders. *American Journal on Intellectual and Developmental Disabilities*, *116*(5), 331–343. https://doi.org/10.1352/1944-7558-116.5.331

Bodfish, J. W., Symons, F. J., Parker, D. E., & Lewis, M. H. (2000). Varieties of Repetitive Behavior in Autism: Comparisons to Mental Retardation. *Journal of Autism and Developmental Disorders*, *30*(3).

Bosl, W. J., Tager-Flusberg, H., & Nelson, C. A. (2018). EEG Analytics for Early Detection of Autism Spectrum Disorder: A data-driven approach. *Scientific Reports*, *8*, 6286. https://doi.org/10.1038/s41598-018-24318-x

Buckner, R. L., Krienen, F. M., Castellanos, A., Diaz, J. C., & Yeo, B. T. T. (2011). The organization of the human cerebellum estimated by intrinsic functional connectivity. *Journal of Neurophysiology*, *106*(5), 2322–2345. https://doi.org/10.1152/jn.00339.2011

Buckner, Randy L. (2013). The cerebellum and cognitive function: 25 years of insight from anatomy and neuroimaging. *Neuron*, *80*(3), 807–815. https://doi.org/10.1016/j.neuron.2013.10.044

Burns, T., King, T., & Spencer, K. (2013). Mullen Scales of Early Learning: The utility in assessing children diagnosed with autism spectrum disorders, cerebral palsy, and epilepsy. *Applied Neuropsychology: Child*, *2*(1).

Carper, R. A., Solders, S., Treiber, J. M., Fishman, I., & Müller, R. A. (2015). Corticospinal tract anatomy and functional connectivity of primary motor cortex in autism. *Journal of the American Academy of Child and Adolescent Psychiatry*, *54*(10), 859–867. https://doi.org/10.1016/j.jaac.2015.07.007

Chawarska, K., Shic, F., Macari, S., Campbell, D. J., Brian, J., Landa, R., Hutman, T., Nelson, C. A., Ozonoff, S., Tager-Flusberg, H., Young, G. S., Zwaigenbaum, L., Cohen, I. L., Charman, T., Messinger, D. S., Klin, A., Johnson, S., & Bryson, S. (2014). 18-month predictors of later outcomes in younger siblings of children with autism spectrum disorder: A baby siblings research consortium study. In *Journal of the American Academy of Child & Adolescent Psychiatry* (Vol. 53, Issue 12, pp. 1317–1327). Elsevier Science.

https://doi.org/10.1016/j.jaac.2014.09.015

Chen, H., Uddin, L. Q., Duan, X., Zheng, J., Long, Z., Zhang, Y., Guo, X., Zhang, Y., Zhao, J., & Chen, H. (2017). Shared atypical default mode and salience network functional connectivity between autism and schizophrenia. *Autism Research : Official Journal of the International Society for Autism Research*, *10*(11), 1776–1786. https://doi.org/10.1002/aur.1834

Constantino, J. N., Zhang, Y., Frazier, T., Abbacchi, A. M., & Law, P. (2010). Sibling recurrence and the genetic epidemiology of autism. *American Journal of Psychiatry*, *167*(11), 1349–1356. https://doi.org/10.1176/appi.ajp.2010.09101470

Crippa, A., Del Vecchio, G., Ceccarelli, S. B., Nobile, M., Arrigoni, F., & Brambilla, P. (2016). Cortico-cerebellar connectivity in Autism Spectrum Disorder: What do we know so far? *Frontiers in Psychiatry*, *7*(FEB), 1–7. https://doi.org/10.3389/fpsyt.2016.00020

D'Mello, A. M., & Stoodley, C. J. (2015). Cerebro-cerebellar circuits in autism spectrum disorder. *Frontiers in Neuroscience*, *9*(NOV). https://doi.org/10.3389/fnins.2015.00408

Das, S., Glatard, T., MacIntyre, L. C., Madjar, C., Rogers, C., Rousseau, M. E., Rioux, P., MacFarlane, D., Mohades, Z., Gnanasekaran, R., Makowski, C., Kostopoulos, P., Adalat, R., Khalili-Mahani, N., Niso, G., Moreau, J. T., & Evans, A. C. (2016). The MNI data-sharing and processing ecosystem. *NeuroImage*, *124*, 1188–1195. https://doi.org/10.1016/j.neuroimage.2015.08.076

Dawson, G., Toth, K., Abbott, R., Osterling, J., Munson, J., Estes, A., & Liaw, J. (2004). Early Social Attention Impairments in Autism: Social Orienting, Joint Attention, and Attention to Distress. *Developmental Psychology*, *40*(2), 271–283. https://doi.org/10.1037/0012-

1649.40.2.271

Dickinson, A., Daniel, M., Marin, A., Gaonkar, B., Dapretto, M., McDonald, N. M., & Jeste, S. (2020). Multivariate Neural Connectivity Patterns in Early Infancy Predict Later Autism Symptoms. *Biological Psychiatry: Cognitive Neuroscience and Neuroimaging*, 1–11. https://doi.org/10.1016/j.bpsc.2020.06.003

Dosenbach, N. U. F., Fair, D. A., Miezin, F. M., Cohen, A. L., Wenger, K. K., Dosenbach, R. A. T., Fox, M. D., Snyder, A. Z., Vincent, J. L., Raichle, M. E., Schlaggar, B. L., & Petersen, S. E. (2007). Distinct brain networks for adaptive and stable task control in humans. *Proceedings of the National Academy of Sciences*, *104*(26), 11073–11078. https://doi.org/10.1073/pnas.0704320104

Dosenbach, Nico U.F., Fair, D. A., Cohen, A. L., Schlaggar, B. L., & Petersen, S. E. (2008). A dual-networks architecture of top-down control. *Trends in Cognitive Sciences*, *12*(3), 99–105. https://doi.org/10.1016/j.tics.2008.01.001

Dosenbach, Nico U.F., Visscher, K. M., Palmer, E. D., Miezin, F. M., Wenger, K. K., Kang, H. C., Burgund, E. D., Grimes, A. L., Schlaggar, B. L., & Petersen, S. E. (2006). A Core System for the Implementation of Task Sets. *Neuron*, *50*(5), 799–812. https://doi.org/10.1016/j.neuron.2006.04.031

Duan, X., Chen, H., He, C., Long, Z., Guo, X., Zhou, Y., Uddin, L. Q., & Chen, H. (2017). Resting-state functional under-connectivity within and between large-scale cortical networks across three low-frequency bands in adolescents with autism. *Progress in Neuro-Psychopharmacology & Biological Psychiatry*, *79*(Pt B), 434–441. https://doi.org/10.1016/j.pnpbp.2017.07.027

Eggebrecht, A. T., Elison, J. T., Feczko, E., Todorov, A., Wolff, J. J., Kandala, S., Adams, C. M., Snyder, A. Z., Lewis, J. D., Estes, A. M., Zwaigenbaum, L., Botteron, K. N., Mckinstry, R. C., Constantino, J. N., Evans, A., Hazlett, H. C., Dager, S., Paterson, S. J., Schultz, R. T., … Chappell, C. (2017). Joint Attention and Brain Functional Connectivity in Infants and Toddlers. *Cerebral Cortex*, *January*, 1–12. https://doi.org/10.1093/cercor/bhw403

Emerson, R. W., Adams, C., Nishino, T., Hazlett, H. C., Wolff, J. J., Zwaigenbaum, L., Constantino, J. N., Shen, M. D., Swanson, M. R., Elison, J. T., Kandala, S., Estes, A. M., Botteron, K. N., Collins, L., Dager, S. R., Evans, A. C., Gerig, G., Gu, H., Mckinstry, R. C., … Piven, J. (2017). Functional neuroimaging of high-risk 6-month-old infants predicts a diagnosis of autism at 24 months of age. *Science Translational Medicine*, *9*(393). https://doi.org/10.1126/scitranslmed.aag2882

Estes, A., Zwaigenbaum, L., Gu, H., St. John, T., Paterson, S., Elison, J. T., Hazlett, H., Botteron, K., Dager, S. R., Schultz, R. T., Kostopoulos, P., Evans, A., Dawson, G., Eliason, J., Alvarez, S., & Piven, J. (2015). Behavioral, cognitive, and adaptive development in infants with autism spectrum disorder in the first 2 years of life. *Journal of Neurodevelopmental Disorders*, *7*(1), 1–10. https://doi.org/10.1186/s11689-015-9117-6

Fatemi, S. H., Aldinger, K. A., Ashwood, P., Bauman, M. L., Blaha, C. D., Blatt, G. J., Chauhan, A., Chauhan, V., Dager, S. R., Dickson, P. E., Estes, A. M., Goldowitz, D., Heck, D. H., Kemper, T. L., King, B. H., Martin, L. A., Millen, K. J., Mittleman, G., Mosconi, M. W., … Welsh, J. P. (2012). Consensus paper: Pathological role of the cerebellum in Autism. *Cerebellum*, *11*(3), 777–807. https://doi.org/10.1007/s12311-012-0355-9

Fearnley, J. M., & Lees, A. J. (1991). Ageing and parkinson's disease: Substantia nigra regional

selectivity. *Brain*, *114*(5), 2283–2301. https://doi.org/10.1093/brain/114.5.2283

Fiez, J. A., Petersen, S. E., Cheney, M. K., & Raichle, M. E. (1992). Impaired non-motor learning and error detection associated with cerebellar damage: A single case study. *Brain*, *115*(1), 155–178. https://doi.org/10.1093/brain/115.1.155

Freedman, E. G., & Foxe, J. J. (2017). Eye movements, sensorimotor adaptation and cerebellar-dependent learning in autism: Toward potential biomarkers and subphenotypes. *European Journal of Neuroscience*, *47*, 549–555. https://doi.org/10.1111/ejn.13625

Gabard-Durnam, L. J., Wilkinson, C., Kapur, K., Tager-Flusberg, H., Levin, A. R., & Nelson, C. A. (2019). Longitudinal EEG power in the first postnatal year differentiates autism outcomes. *Nature Communications*, *10*(1). https://doi.org/10.1038/s41467-019-12202-9

Gardner, W., Mulvey, E. P., & Shaw, E. C. (1995). Regression analyses of counts and rates: Poisson, overdispersed Poisson, and negative binomial models. In *Psychological Bulletin* (Vol. 118, Issue 3, pp. 392–404). American Psychological Association. https://doi.org/10.1037/0033-2909.118.3.392

Gholipour, A., Kehtarnavaz, N., Gopinath, K., Briggs, R., & Panahi, I. (2008). Average field map image template for Echo-Planar image analysis. *Annual International Conference of the IEEE Engineering in Medicine and Biology Society. IEEE Engineering in Medicine and Biology Society. Annual International Conference*, *2008*, 94–97. https://doi.org/10.1109/IEMBS.2008.4649099

Gotham, K., Pickles, A., & Lord, C. (2009). Standardizing ADOS scores for a measure of severity in autism spectrum disorders. *Journal of Autism and Developmental Disorders*, *39*(5), 693–705. https://doi.org/10.1007/s10803-008-0674-3

Grady, C., Sarraf, S., Saverino, C., & Campbell, K. (2016). Age differences in the functional interactions among the default, frontoparietal control, and dorsal attention networks. *Neurobiology of Aging*, *41*, 159–172. https://doi.org/10.1016/j.neurobiolaging.2016.02.020

Green, P., & Macleod, C. J. (2016). SIMR: An R package for power analysis of generalized linear mixed models by simulation. *Methods in Ecology and Evolution*, *7*(4), 493–498. https://doi.org/10.1111/2041-210X.12504

Guo, X., Duan, X., Suckling, J., Chen, H., Liao, W., Cui, Q., & Chen, H. (2019). Partially impaired functional connectivity states between right anterior insula and default mode network in autism spectrum disorder. *Human Brain Mapping*, *40*(4), 1264–1275. https://doi.org/10.1002/hbm.24447

Hampson, D. R., & Blatt, G. J. (2015). Autism spectrum disorders and neuropathology of the cerebellum. *Frontiers in Neuroscience*, *9*(NOV), 1–16. https://doi.org/10.3389/fnins.2015.00420

Hanaie, R., Mohri, I., Kagitani-Shimono, K., Tachibana, M., Matsuzaki, J., Hirata, I., Nagatani, F., Watanabe, Y., Katayama, T., & Taniike, M. (2018). Aberrant cerebellar–cerebral functional connectivity in children and adolescents with autism spectrum disorder. *Frontiers in Human Neuroscience*, *12*(November), 1–13. https://doi.org/10.3389/fnhum.2018.00454

Hazlett, H. C., Gu, H., Munsell, B. C., Kim, S. H., Styner, M., Wolff, J. J., Elison, J. T., Swanson, M. R., Zhu, H., Botteron, K. N., Collins, D. L., Constantino, J. N., Dager, S. R., Estes, A. M., Evans, A. C., Fonov, V. S., Gerig, G., Kostopoulos, P., McKinstry, R. C., … Piven, J. (2017). Early brain development in infants at high risk for autism spectrum

disorder. *Nature*, *542*(7641), 348–351. https://doi.org/10.1038/nature21369

Hoche, F., Guell, X., Sherman, J. C., Vangel, M. G., & Schmahmann, J. D. (2016). Cerebellar Contribution to Social Cognition. *Cerebellum*, *15*(6), 732–743. https://doi.org/10.1007/s12311-015-0746-9

Hus, V., Gotham, K., & Lord, C. (2014). Standardizing ADOS domain scores: separating severity of social affect and restricted and repetitive behaviors. *Journal of Autism and Developmental Disorders*, *44*(10), 2400–2412. https://doi.org/10.1007/s10803-012-1719-1

Jones, W., & Klin, A. (2013). Attention to eyes is present but in decline in 2-6-month-old infants later diagnosed with autism. *Nature*, *504*(7480), 427–431. https://doi.org/10.1038/nature12715

Jung, M., Kosaka, H., Saito, D. N., Ishitobi, M., Morita, T., Inohara, K., Asano, M., Arai, S., Munesue, T., Tomoda, A., Wada, Y., Sadato, N., Okazawa, H., & Iidaka, T. (2014). Default mode network in young male adults with autism spectrum disorder: Relationship with autism spectrum traits. *Molecular Autism*, *5*(1), 1–11. https://doi.org/10.1186/2040-2392-5-35

Keown, C. L., Datko, M. C., Chen, C. P., Maximo, J. O., Jahedi, A., & Müller, R. A. (2017). Network Organization Is Globally Atypical in Autism: A Graph Theory Study of Intrinsic Functional Connectivity. *Biological Psychiatry: Cognitive Neuroscience and Neuroimaging*, *2*(1), 66–75. https://doi.org/10.1016/j.bpsc.2016.07.008

Khan, A. J., Nair, A., Keown, C. L., Datko, M. C., Lincoln, A. J., & Müller, R.-A. (2015). Cerebro-cerebellar resting state functional connectivity in children and adolescents with autism spectrum disorder. *Biological Psychiatry*, *78*(9).

https://doi.org/10.1016/j.biopsych.2015.03.024

Lam, K. S. L., & Aman, M. G. (2007). The repetitive behavior scale-revised: Independent validation in individuals with autism spectrum disorders. *Journal of Autism and Developmental Disorders*, *37*(5), 855–866. https://doi.org/10.1007/s10803-006-0213-z

Lawrence, K. E., Hernandez, L. M., Bookheimer, S. Y., & Dapretto, M. (2019). Atypical Longitudinal Development of Functional Connectivity in Adolescents with Autism Spectrum Disorder. *Autism Research*, *12*(1), 53–65. https://doi.org/10.1145/3369457.3370914

Leggio, M., & Molinari, M. (2015). Cerebellar Sequencing: a Trick for Predicting the Future. *Cerebellum*, *14*(1), 35–38. https://doi.org/10.1007/s12311-014-0616-x

Limperopoulos, C., Bassan, H., Gauvreau, K., Robertson, R. L., Sullivan, N. R., Benson, C. B., Avery, L., Stewart, J., Soul, J. S., Ringer, S. A., Volpe, J. J., & Du Plessis, A. J. (2007). Does cerebellar injury in premature infants contribute to the high prevalence of long-term cognitive, learning, and behavioral disability in survivors? *Pediatrics*, *120*(3), 584–593. https://doi.org/10.1542/peds.2007-1041

Lord, C., Rutter, M., DiLavore, P., Risi, S., Gotham, K., & Bishop, S. (2001). *Autism diagnostic observation schedule (ADOS): Manual*. WPS.

Manto, M., Gruol, D. L., Schmahmann, J. D., Koibuchi, N., & Rossi, F. (2013). Handbook of the cerebellum and cerebellar disorders. *Handbook of the Cerebellum and Cerebellar Disorders*, *January 2013*, 1–2424. https://doi.org/10.1007/978-94-007-1333-8

Marek, S., & Dosenbach, N. U. F. (2018). The frontoparietal network: function, electrophysiology, and importance of individual precision mapping. *Dialogues Clin*

Neurosci, *20*, 133–140. www.dialogues-cns.org

Marek, S., Siegel, J. S., Gordon, E. M., Raut, R. V., Gratton, C., Newbold, D. J., Ortega, M., Laumann, T. O., Miller, D. B., Zheng, A., Lopez, K. C., Berg, J. J., Coalson, R. S., Nguyen, A. L., Dierker, D., Van, A. N., Hoyt, C. R., McDermott, K. B., Norris, S. A., … Dosenbach, N. U. F. (2018). Spatial and Temporal Organization of the Individual Human Cerebellum. *Neuron*, 1–17. https://doi.org/10.2139/ssrn.3188429

Marek, S., Tervo-Clemmens, B., Calabro, F. J., Montez, D. F., Kay, B. P., Hatoum, A. S., Rose Donohue, M., Foran, W., Miller, R. L., Feczko, E., Miranda-Dominguez, O., Graham, A. M., Chen, J., Newbold, D. J., Zheng, A., Seider, N. A., Van, A. N., Laumann, T. O., Thompson, W. K., … Dosenbach, N. (2020). Towards Reproducible Brain-Wide Association Studies. *BioRxiv*, *11*, 15–18. https://doi.org/10.1101/2020.08.21.257758

Marko, M. K., Crocetti, D., Hulst, T., Donchin, O., Shadmehr, R., & Mostofsky, S. H. (2015). Behavioural and neural basis of anomalous motor learning in children with autism. *Brain*, *138*(3), 784–797. https://doi.org/10.1093/brain/awu394

Marrus, N., Eggebrecht, A. T., Todorov, A., Elison, J. T., Wolff, J. J., Cole, L., Gao, W., Pandey, J., Shen, M. D., Swanson, M. R., Emerson, R. W., Klohr, C. L., Adams, C. M., Estes, A. M., Zwaigenbaum, L., Botteron, K. N., Mckinstry, R. C., Constantino, J. N., Evans, A. C., … Das, S. (2018). Walking, Gross Motor Development, and Brain Functional Connectivity in Infants and Toddlers. *Cerebral Cortex*, 1–14. https://doi.org/10.1093/cercor/bhx313

Mash, L. E., Linke, A. C., Olson, L. A., Fishman, I., Liu, T. T., & Müller, R. A. (2019). Transient states of network connectivity are atypical in autism: A dynamic functional connectivity study. *Human Brain Mapping*, *40*(8), 2377–2389.

https://doi.org/10.1002/hbm.24529

May, T., McGinley, J., Murphy, A., Hinkley, T., Papadopoulos, N., Williams, K. J., McGillivray, J., Enticott, P. G., Leventer, R. J., & Rinehart, N. J. (2016). A Multidisciplinary Perspective on Motor Impairment as an Early Behavioural Marker in Children with Autism Spectrum Disorder. *Australian Psychologist*, *51*(4), 296–303. https://doi.org/10.1111/ap.12225

McKinnon, C. J., Eggebrecht, A. T., Todorov, A., Wolff, J. J., Elison, J. T., Adams, C. M., Snyder, A. Z., Estes, A. M., Zwaigenbaum, L., Botteron, K. N., McKinstry, R. C., Marrus, N., Evans, A., Hazlett, H. C., Dager, S. R., Paterson, S. J., Pandey, J., Schultz, R. T., Styner, M. A., … Pruett, J. R. (2019). Restricted and Repetitive Behavior and Brain Functional Connectivity in Infants at Risk for Developing Autism Spectrum Disorder. *Biological Psychiatry: Cognitive Neuroscience and Neuroimaging*, *4*(1), 50–61. https://doi.org/10.1016/j.bpsc.2018.09.008

Menon, V. (2018). The Triple Network Model, Insight, and Large-Scale Brain Organization in Autism. *Biological Psychiatry*, *84*(4), 236–238. https://doi.org/10.1016/j.biopsych.2018.06.012

Mirenda, P., Smith, I. M., Vaillancourt, T., Georgiades, S., Duku, E., Szatmari, P., Bryson, S., & Fombonne, E. (2010). *Validating the Repetitive Behavior Scale-Revised in Young Children with Autism Spectrum Disorder*. 1521–1530. https://doi.org/10.1007/s10803-010-1012-0

Moberget, T., & Ivry, R. B. (2016). Cerebellar contributions to motor control and language comprehension: searching for common computational principles. *Ann N Y Acad Sci*, *1360*(1), 154–171. https://doi.org/10.1111/nyas.13094.Cerebellar

Mullen, E. (1995). *Mullen Scales of Early Learning*. AGS. https://doi.org/10.1007/978-0-387-

79948-3_1570

Nair, A., Jolliffe, M., Lograsso, Y. S. S., & Bearden, C. E. (2020). A Review of Default Mode Network Connectivity and Its Association With Social Cognition in Adolescents With Autism Spectrum Disorder and Early-Onset Psychosis. *Frontiers in Psychiatry*, *11*(June), 1–17. https://doi.org/10.3389/fpsyt.2020.00614

Neta, M., Schlaggar, B. L., & Petersen, S. E. (2014). NeuroImage Separable responses to error , ambiguity , and reaction time in cingulo-opercular task control regions. *NeuroImage*, *99*, 59–68. https://doi.org/10.1016/j.neuroimage.2014.05.053

Nielsen, A. N., Greene, D. J., Gratton, C., Dosenbach, N. U. F., Petersen, S. E., & Schlaggar, B. L. (2019). Evaluating the Prediction of Brain Maturity from Functional Connectivity after Motion Artifact Denoising. *Cerebral Cortex*, *29*(6), 2455–2469. https://doi.org/10.1093/cercor/bhy117

Ojemann, J. G., Akbudak, E., Snyder, A. Z., McKinstry, R. C., Raichle, M. E., & Conturo, T. E. (1997). Anatomic localization and quantitative analysis of gradient refocused echo-planar fMRI susceptibility artifacts. *NeuroImage*, *6*(3), 156–167. https://doi.org/10.1006/nimg.1997.0289

Oldehinkel, M., Mennes, M., Marquand, A., Charman, T., Tillmann, J., Ecker, C., Dell'Acqua, F., Brandeis, D., Banaschewski, T., Baumeister, S., Moessnang, C., Baron-Cohen, S., Holt, R., Bölte, S., Durston, S., Kundu, P., Lombardo, M. V., Spooren, W., Loth, E., … Zwiers, M. P. (2019). Altered Connectivity Between Cerebellum, Visual, and Sensory-Motor Networks in Autism Spectrum Disorder: Results from the EU-AIMS Longitudinal European Autism Project. *Biological Psychiatry: Cognitive Neuroscience and Neuroimaging*, *4*(3),

260–270. https://doi.org/10.1016/j.bpsc.2018.11.010

Ozonoff, S, Young, G., Carter, A., Messinger, D., Yirmiya, N., Zwaigenbaum, L., Bryson, S., Carver, L., Constantino, J., Dobkins, K., Hutman, T., Iverson, J., Landa, R., Rogers, S., Sigman, M., & Stone, W. (2011). Recurrence risk for autism spectrum disorders: A baby siblings research consortium study. *Pediatrics*, *128*(3), e488–e495. https://doi.org/peds.2010-2825 [pii]\r10.1542/peds.2010-2825

Ozonoff, Sally, Iosif, A.-M., Baguio, F., Cook, I., Moore Hill, M., Hutman, T., Rogers, S., Rozga, A., Sangha, S., Sigman, M., Steinfeld, M. B., & Young, G. (2010). A Prospective Study of the Emergence of Early Behavioral Signs of Autism. *Journal of the American Academy of Child & Adolescent Psychiatry*, *49*(3), 256–266. https://doi.org/10.1016/j.jaac.2009.11.009

Padmanabhan, A., Lynch, C. J., Schaer, M., & Menon, V. (2017). Defaul mode network in Autism. *Biol Psychiatry Cogn Neurosci Neuroimaging*, *2*(6), 476–486. https://doi.org/10.1016/j.bpsc.2017.04.004.The

Padmanabhan, A., Lynn, A., Foran, W., Luna, B., & O'Hearn, K. (2013). Age related changes in striatal resting state functional connectivity in autism. *Frontiers in Human Neuroscience*, *7*(November), 1–16. https://doi.org/10.3389/fnhum.2013.00814

Park, D. C., & Reuter-Lorenz, P. (2009). The Adaptive Brain: Aging and Neurocognitive Scaffolding. *Annual Review of Psychology*, *60*(1), 173–196. https://doi.org/10.1146/annurev.psych.59.103006.093656

Pedregosa, F., Varoquaux, G., Gramfort, A., Michel, V., Thirion, B., Grisel, O., Blondel, M., Prettenhofer, P., Weiss, R., Dubourg, V., Vanderplas, J., Passos, A., Cournapeau, D.,

Brucher, M., Perrot, M., & Duchesnay, É. (2011). Scikit-learn: Machine Learning in Python. *Journal of Machine Learning Research*, *12*(85), 2825–2830. http://jmlr.org/papers/v12/pedregosa11a.html

Peterburs, J., & Desmond, J. E. (2016). The role of the human cerebellum in performance monitoring. *Current Opinion in Neurobiology*, *40*, 38–44. https://doi.org/10.1016/j.conb.2016.06.011

Piven, J., Elison, J. T., & Zylka, M. J. (2017). Toward a conceptual framework for early brain and behavior development in Autism. *Molecular Psychiatry*, *22*(10), 1–10. https://doi.org/10.1038/mp.2017.131

Power, J. D., & Petersen, S. E. (2013). Control-related systems in the human brain. *Current Opinion in Neurobiology*, *23*(2), 223–228. https://doi.org/10.1016/j.conb.2012.12.009

Pruett, J. R., Kandala, S., Hoertel, S., Snyder, A. Z., Elison, J. T., Nishino, T., Feczko, E., Dosenbach, N. U. F., Nardos, B., Power, J. D., Adeyemo, B., Botteron, K. N., McKinstry, R. C., Evans, A. C., Hazlett, H. C., Dager, S. R., Paterson, S., Schultz, R. T., Collins, D. L., … Piven, J. (2015). Accurate age classification of 6 and 12 month-old infants based on resting-state functional connectivity magnetic resonance imaging data. *Developmental Cognitive Neuroscience*, *12*, 123–133. https://doi.org/10.1016/j.dcn.2015.01.003

R Core Team. (2018). *R: A language and environment for statistical computing.* R Foundation for Statistical Computing.

Ramos, T. C., Balardin, J. B., Sato, J. R., & Fujita, A. (2019). Abnormal cortico-cerebellar functional connectivity in autism spectrum disorder. *Frontiers in Systems Neuroscience*, *12*(January). https://doi.org/10.3389/fnsys.2018.00074

Ringnér, M. (2008). What is principal component analysis? *Nature Biotechnology*, *26*(3), 303–304. https://doi.org/10.1038/nbt0308-303

Robins, D. L., Fein, D., Barton, M. L., & Green, J. A. (2001). The Modified Checklist for Autism in Toddlers: an initial study investigating the early detection of autism and pervasive developmental disorders. *Journal of Autism and Developmental Disorders*, *31*(2), 131–144.

Rogers, T. D., McKimm, E., Dickson, P. E., Goldowitz, D., Blaha, C. D., & Mittleman, G. (2013). Is autism a disease of the cerebellum? An integration of clinical and pre-clinical research. *Frontiers in Systems Neuroscience*, *7*(May), 1–16. https://doi.org/10.3389/fnsys.2013.00015

Rosen, M. L., Amso, D., & McLaughlin, K. A. (2019). The role of the visual association cortex in scaffolding prefrontal cortex development: A novel mechanism linking socioeconomic status and executive function. *Developmental Cognitive Neuroscience*, *39*(July), 100699. https://doi.org/10.1016/j.dcn.2019.100699

Rosvall, M., & Bergstrom, C. T. (2007). *Maps of random walks on complex networks reveal community structure*. *105*(4). https://doi.org/10.1073/pnas.0706851105

Rutter, M., Bailey, A., & Lord, C. (2003). *The social communication questionnaire: Manual*. Western Psychological Services.

Schmahmann, J. D., & Sherman, J. C. (1998). The cerebellar cognitive affective syndrome. *Brain*, *121*(4), 561–579. https://doi.org/10.1093/brain/121.4.561

Seitzman, B. A., Gratton, C., Marek, S., Raut, R. V., Dosenbach, N. U. F., Schlaggar, B. L., Petersen, S. E., & Greene, D. J. (2020). A set of functionally-defined brain regions with

improved representation of the subcortex and cerebellum. *NeuroImage*, *206*(July 2019), 116290. https://doi.org/10.1016/j.neuroimage.2019.116290

Shen, M., & Piven, J. (2017). Brain and behavior development in autism from birth through infancy. *Dialogues in Clinical Neuroscience*, *19*(4), 325.

Sinha, P., Kjelgaard, M. M., Gandhi, T. K., Tsourides, K., Cardinaux, A. L., Pantazis, D., Diamond, S. P., & Held, R. M. (2014). Autism as a disorder of prediction. *Proceedings of the National Academy of Sciences*, *111*(42), 15220–15225. https://doi.org/10.1073/pnas.1416797111

Sokolov, A. A., Miall, R. C., & Ivry, R. B. (2017). The Cerebellum: Adaptive Prediction for Movement and Cognition. *Trends in Cognitive Sciences*, *21*(5), 313–332. https://doi.org/10.1016/j.tics.2017.02.005

Van Rossum, G., & Drake Jr, F. L. (1995). *Python tutorial*. Centrum voor Wiskunde en Informatica Amsterdam, The Netherlands.

Verly, M., Verhoeven, J., Zink, I., Mantini, D., Peeters, R., Deprez, S., Emsell, L., Boets, B., Noens, I., Steyaert, J., Lagae, L., De Cock, P., Rommel, N., & Sunaert, S. (2014). Altered functional connectivity of the language network in ASD: Role of classical language areas and cerebellum. *NeuroImage: Clinical*, *4*, 374–382. https://doi.org/10.1016/j.nicl.2014.01.008

Wang, S. S. H., Kloth, A. D., & Badura, A. (2014). The Cerebellum, Sensitive Periods, and Autism. *Neuron*, *83*(3), 518–532. https://doi.org/10.1016/j.neuron.2014.07.016

Werchan, D., & Amso, D. (2017). A Novel Ecological Account of Prefrontal Cortex Functional Development. *Psychol. Review*, *124*(6), 139–148. https://doi.org/10.1037/rev0000078.A

Wetherby, A., Allen, L., Cleary, J., Kublin, K., & Goldstein, H. (2002). Validity and reliability of the communication and symbolic behavior scales developmental profile with very young children. *Journal of Speech, Language, and Hearing Research*, *45*, 1202–121.

Wheelock, M. D., Austin, N. C., Bora, S., Eggebrecht, A. T., Melzer, T. R., Woodward, L. J., & Smyser, C. D. (2018). Altered functional network connectivity relates to motor development in children born very preterm. *NeuroImage*, *183*(May), 574–583. https://doi.org/10.1016/j.neuroimage.2018.08.051

Wickham, H., Averick, M., Bryan, J., Chang, W., McGowan, L., François, R., Grolemund, G., Hayes, A., Henry, L., Hester, J., Kuhn, M., Pedersen, T., Miller, E., Bache, S., Müller, K., Ooms, J., Robinson, D., Seidel, D., Spinu, V., … Yutani, H. (2019). Welcome to the Tidyverse. *Journal of Open Source Software*, *4*(43), 1686. https://doi.org/10.21105/joss.01686

Wolf, U., Rapoport, M. J., & Schweizer, T. A. (2009). Evaluating the affective component of the cerebellar cognitive affective syndrome. *Journal of Neuropsychiatry and Clinical Neurosciences*, *21*(3), 245–253. https://doi.org/10.1176/jnp.2009.21.3.245

Wolff, J. J., Botteron, K. N., Dager, S. R., Elison, J. T., Estes, A. M., Gu, H., Hazlett, H. C., Pandey, J., Paterson, S. J., Schultz, R. T., Zwaigenbaum, L., & Piven, J. (2014). Longitudinal patterns of repetitive behavior in toddlers with autism. *Journal of Child Psychology and Psychiatry and Allied Disciplines*, *55*(8), 945–953. https://doi.org/10.1111/jcpp.12207

Wolff, J. J., & Piven, J. (2020). Predicting Autism Risk in Infancy. In *Journal of the American Academy of Child & Adolescent Psychiatry*. American Academy of Child & Adolescent

Psychiatry. https://doi.org/10.1016/j.jaac.2020.07.910

Wolff, J. J., Swanson, M. R., Elison, J. T., Gerig, G., Pruett, J. R., Styner, M. A., Vachet, C., Botteron, K. N., Dager, S. R., Estes, A. M., Hazlett, H. C., Schultz, R. T., Shen, M. D., Zwaigenbaum, L., & Piven, J. (2017). Neural circuitry at age 6 months associated with later repetitive behavior and sensory responsiveness in autism. *Molecular Autism*. https://doi.org/10.1186/s13229-017-0126-z

Zwaigenbaum, L., Bryson, S., Rogers, T., Roberts, W., Brian, J., & Szatmari, P. (2005). Behavioral manifestations of autism in the first year of life. *International Journal of Developmental Neuroscience*, *23*(2-3 SPEC. ISS.), 143–152. https://doi.org/10.1016/j.ijdevneu.2004.05.001

Appendix

Appendix A. ROI coordinates (Talairach [X, Y, Z] and MNI [X, Y, Z]) and network assignments across development. Networks were derived in 6-month infants (6M-Net; present results), 12 and 24-month toddlers (12_24M_Net; Eggebrecht et al., 2017), and adults (Adult_230_Net; Power et al., 2011). Cerebellar ROIs 231 and 234 were placed by reverse seeding the DMN in the right and left hemispheres, respectively; cerebellar ROIs 232 and 233 were placed by reverse seeding the FPN in the right and left hemispheres, respectively (see Appendix B for additional details about cerebellar ROI placement).

Key	Talairach			MNI			Network Solution			CBM_ROI
	X	Y	Z	X	Y	Z	6M	12-24M	Adult	
1	-23.00	-96.00	-15.00	-24.66	-97.84	-12.33	VIS	DAN	US	0
2	26.00	-96.00	-15.00	26.68	-97.30	-13.49	VIS	DAN	US	0
3	23.00	27.00	-12.00	23.96	31.94	-17.78	aFP	aFPC	US	0
4	-53.00	-45.00	-24.00	-56.16	-44.76	-24.23	DAN	DAN	US	0
5	8.00	36.00	-18.00	8.13	41.12	-24.31	aFP	aFPC	US	0
6	-20.00	-24.00	-18.00	-21.38	-22.22	-19.97	mVIS	pcDMN	DMN	0
7	-35.00	-30.00	-24.00	-37.26	-28.80	-25.58	DAN	DAN	US	0
8	62.00	-27.00	-15.00	64.60	-24.41	-18.57	tDMN	pFPC	DMN	0
9	50.00	-36.00	-24.00	51.79	-34.17	-27.23	DAN	DAN	US	0
10	53.00	-33.00	-14.00	55.18	-30.80	-16.93	tDMN	pFPC	US	0
11	32.00	33.00	-6.00	33.55	38.46	-12.03	aFP	Sal	FPC	0
12	-8.00	-54.00	57.00	-7.12	-52.22	60.71	SM1	SMN	Sal	0
13	8.00	-6.00	45.00	9.50	-1.84	44.73	SM1	SMN	Mot	0
14	-8.00	-24.00	63.00	-6.90	-20.59	65.21	SM1	SMN	Mot	0
15	-8.00	-36.00	69.00	-6.79	-33.09	72.27	SM1	SMN	Mot	0
16	-52.00	-25.00	41.00	-53.52	-22.54	43.10	SM2	SMN2	Mot	0
17	8.00	-48.00	69.00	9.94	-45.52	72.63	SM1	SMN	Mot	0
18	-39.00	-22.00	52.00	-39.63	-19.04	54.21	SM2	SMN	Mot	0
19	26.00	-42.00	57.00	28.54	-39.24	59.17	SM2	SMN2	Mot	0
20	47.00	-24.00	42.00	50.24	-20.37	41.74	SM2	SMN2	Mot	0
21	18.00	-32.00	58.00	20.21	-28.80	59.80	SM1	SMN	Mot	0
22	-29.00	-45.00	57.00	-29.10	-43.00	60.66	SM2	SMN2	Mot	0
23	20.00	-45.00	66.00	22.45	-42.29	68.99	SM1	SMN	Mot	0
24	-44.00	-34.00	44.00	-45.10	-31.85	46.63	SM2	SMN2	DAN	0
25	-21.00	-34.00	58.00	-20.66	-31.33	60.85	SM1	SMN	Mot	0
26	39.00	-24.00	54.00	42.14	-20.24	54.59	SM2	SMN2	Mot	0
27	35.00	-21.00	45.00	37.74	-17.30	45.01	SM2	SMN	Mot	0
28	-48.00	-14.00	34.00	-49.47	-11.06	34.95	MotM	CO	MotM	0
29	34.00	-13.00	16.00	36.04	-9.44	13.95	MotM	CO	MotM	0
30	48.00	-10.00	34.00	51.14	-5.80	32.42	MotM	CO	MotM	0
31	-51.00	-13.00	24.00	-52.84	-10.23	24.41	MotM	CO	MotM	0

32	62.00	-12.00	27.00	65.64	-7.88	24.83	MotM	CO	MotM	0
33	-4.00	-2.00	53.00	-2.88	2.38	53.21	CO	SMN	Mot	0
34	51.00	-31.00	34.00	54.22	-27.83	33.64	SM2	SMN2	CO	0
35	17.00	-12.00	63.00	19.33	-7.71	63.88	SM1	SMN	Mot	0
36	-11.00	-6.00	42.00	-10.48	-2.10	42.02	SM1	SMN	Mot	0
37	35.00	-3.00	0.00	36.73	0.78	-3.57	CO	CO	Mot	0
38	5.00	3.00	51.00	6.52	7.69	50.58	CO	SMN	Mot	0
39	-43.00	-3.00	10.00	-44.76	0.10	8.83	CO	CO	Mot	0
40	47.00	4.00	3.00	49.40	8.32	-1.12	CO	CO	Mot	0
41	-33.00	0.00	6.00	-34.37	3.29	4.19	CO	CO	Mot	0
42	-6.00	13.00	36.00	-5.33	17.80	34.41	CO	SMN	Sal	0
43	34.00	6.00	5.00	35.83	10.32	1.18	CO	CO	Sal	0
44	62.00	-36.00	21.00	65.43	-33.20	19.97	SM2	pCO	CO	0
45	55.00	-19.00	10.00	57.88	-15.62	7.49	pCO	pCO	CO	0
46	-37.00	-35.00	16.00	-38.43	-33.34	16.98	pCO	pCO	CO	0
47	-58.00	-27.00	13.00	-60.48	-25.22	13.82	pCO	pCO	CO	0
48	-47.00	-28.00	5.00	-49.14	-26.30	5.18	tDMN	tDMN	CO	0
49	41.00	-26.00	21.00	43.45	-22.93	19.85	SM2	pCO	Mot	0
50	-48.00	-36.00	24.00	-49.77	-34.36	25.74	SM2	pCO	CO	0
51	-51.00	-24.00	22.00	-52.92	-21.83	22.97	SM2	SMN2	Mot	0
52	-53.00	-12.00	12.00	-55.22	-9.42	11.73	MotM	CO	CO	0
53	53.00	-9.00	16.00	55.96	-5.03	13.25	MotM	CO	CO	0
54	56.00	-21.00	30.00	59.40	-17.34	28.69	SM2	SMN2	Mot	0
55	-29.00	-29.00	12.00	-30.12	-27.02	12.20	SM1	pCO	SubCtx	0
56	-39.00	-75.00	22.00	-40.50	-75.27	25.80	pDMN	pcDMN	DMN	0
57	5.00	60.00	3.00	5.55	66.69	-3.55	aDMN	aFPC	DMN	0
58	8.00	42.00	-9.00	8.36	47.59	-15.18	aDMN	aDMN	DMN	0
59	-17.00	57.00	-3.00	-17.65	63.19	-9.17	aFP	aFPC	US	0
60	-44.00	-61.00	18.00	-45.79	-60.69	20.85	tDMN	tDMN	DMN	0
61	41.00	-73.00	26.00	43.43	-72.21	28.00	pDMN	pcDMN	DMN	0
62	-41.00	9.00	-30.00	-43.58	11.99	-34.15	tDMN	tDMN	DMN	0
63	44.00	12.00	-24.00	45.64	16.20	-30.02	tDMN	tDMN	DMN	0
64	-55.00	-27.00	-14.00	-57.97	-25.69	-14.73	tDMN	pFPC	US	0
65	26.00	12.00	-12.00	27.06	16.22	-16.93	aDMN	aDMN	DMN	0
66	-43.00	-65.00	31.00	-44.45	-64.64	34.78	pDMN	pcDMN	DMN	0
67	-7.00	-56.00	25.00	-6.84	-54.90	27.05	pDMN	pcDMN	DMN	0
68	5.00	-60.00	33.00	5.91	-58.82	35.45	pDMN	pcDMN	DMN	0
69	-11.00	-57.00	14.00	-11.29	-56.20	15.60	pDMN	pcDMN	DMN	0
70	-3.00	-50.00	12.00	-2.94	-48.79	12.87	pDMN	pcDMN	DMN	0
71	7.00	-50.00	29.00	7.94	-48.37	30.57	pDMN	tDMN	DMN	0
72	14.00	-64.00	24.00	15.12	-63.09	25.98	pDMN	pcDMN	DMN	0
73	-3.00	-39.00	42.00	-2.20	-36.68	43.85	pDMN	pcDMN	DMN	0
74	10.00	-55.00	16.00	10.77	-53.83	17.09	pDMN	pcDMN	DMN	0
75	49.00	-61.00	34.00	52.04	-59.37	35.52	tDMN	pFPC	DMN	0
76	21.00	27.00	50.00	23.33	33.07	47.68	aDMN	aDMN	DMN	0
77	-17.00	23.00	54.00	-16.40	28.52	53.05	aDMN	aDMN	DMN	0
78	20.00	33.00	42.00	22.11	39.21	38.90	aDMN	aDMN	DMN	0
79	-20.00	39.00	42.00	-19.78	45.07	39.48	aDMN	aDMN	DMN	0
80	5.00	48.00	21.00	5.94	54.42	16.18	aDMN	aDMN	DMN	0
81	-7.00	45.00	4.00	-7.04	50.82	-1.29	aDMN	aDMN	DMN	0
82	8.00	48.00	9.00	8.80	54.23	3.45	aDMN	aDMN	DMN	0
83	-3.00	39.00	-4.00	-3.06	44.41	-9.46	aDMN	aDMN	DMN	0
84	7.00	37.00	0.00	7.51	42.49	-5.35	aDMN	aDMN	DMN	0
85	-11.00	39.00	12.00	-11.06	44.62	7.61	aDMN	aDMN	DMN	0
86	-3.00	32.00	39.00	-2.06	37.85	36.34	aDMN	aDMN	FPC	0
87	-3.00	36.00	20.00	-2.50	41.70	16.05	aDMN	aDMN	DMN	0

88	-8.00	42.00	27.00	-7.55	48.08	23.18	aDMN	aDMN	DMN	0
89	62.00	-15.00	-15.00	64.64	-11.80	-19.30	tDMN	tDMN	DMN	0
90	-53.00	-15.00	-9.00	-55.72	-12.96	-10.24	tDMN	tDMN	DMN	0
91	-55.00	-31.00	-4.00	-57.75	-29.70	-3.94	tDMN	tDMN	DMN	0
92	62.00	-33.00	-6.00	64.80	-30.55	-8.70	tDMN	pFPC	FPC	0
93	11.00	30.00	24.00	12.25	35.63	20.30	aDMN	aDMN	DMN	0
94	50.00	-6.00	-12.00	52.16	-2.43	-16.40	tDMN	tDMN	DMN	0
95	-25.00	-41.00	-8.00	-26.44	-39.95	-8.26	mVIS	pcDMN	DMN	0
96	26.00	-39.00	-11.00	26.94	-37.34	-12.76	mVIS	pcDMN	DMN	0
97	-32.00	-39.00	-15.00	-33.93	-38.06	-15.60	mVIS	pcDMN	DMN	0
98	28.00	-76.00	-31.00	28.46	-76.56	-31.64	VIS	CO	DMN	1
99	50.00	3.00	-24.00	51.90	6.81	-29.61	tDMN	tDMN	DMN	0
100	-50.00	0.00	-24.00	-52.89	2.55	-27.06	tDMN	tDMN	DMN	0
101	44.00	-52.00	28.00	46.68	-50.08	28.76	pDMN	tDMN	DMN	0
102	-47.00	-43.00	0.00	-49.30	-42.15	0.83	tDMN	tDMN	DMN	0
103	-29.00	15.00	-15.00	-30.63	18.71	-18.98	aDMN	aDMN	DMN	0
104	-3.00	-37.00	30.00	-2.47	-34.80	31.07	pDMN	pcDMN	DMN	0
105	-7.00	-72.00	38.00	-6.58	-71.47	41.74	pDMN	pcDMN	DMN	0
106	10.00	-67.00	39.00	11.27	-66.01	42.09	pDMN	pFPC	DMN	0
107	3.00	-50.00	48.00	4.20	-48.06	50.71	pDMN	pcDMN	DMN	0
108	-44.00	27.00	-9.00	-46.17	31.26	-13.03	aFP	Sal	DMN	0
109	47.00	30.00	-6.00	49.26	35.47	-12.20	aFP	Sal	DMN	0
110	8.00	-90.00	-9.00	7.98	-91.08	-7.10	VIS	DAN	Vis	0
111	17.00	-90.00	-15.00	17.27	-91.09	-13.64	VIS	DAN	US	0
112	-11.00	-93.00	-15.00	-12.08	-94.56	-12.80	VIS	DAN	US	0
113	17.00	-48.00	-9.00	17.53	-46.86	-9.88	mVIS	Vis	Vis	0
114	38.00	-73.00	13.00	39.98	-72.49	14.36	mVIS	pcDMN	Vis	0
115	8.00	-72.00	9.00	8.45	-71.84	10.79	mVIS	Vis	Vis	0
116	-8.00	-80.00	5.00	-8.43	-80.50	7.44	mVIS	Vis	Vis	0
117	-27.00	-79.00	16.00	-28.07	-79.45	19.43	mVIS	DAN	Vis	0
118	19.00	-66.00	1.00	19.81	-65.56	1.72	mVIS	Vis	Vis	0
119	-23.00	-90.00	15.00	-23.94	-90.98	18.96	mVIS	DAN	Vis	0
120	26.00	-60.00	-9.00	26.93	-59.37	-9.36	mVIS	DAN	Vis	0
121	-14.00	-72.00	-9.00	-15.02	-72.42	-7.68	mVIS	Vis	Vis	0
122	-17.00	-68.00	3.00	-17.87	-68.03	4.81	mVIS	Vis	Vis	0
123	41.00	-78.00	-12.00	42.52	-78.17	-11.78	DAN	DAN	Vis	0
124	-44.00	-75.00	-12.00	-46.54	-75.95	-9.95	DAN	DAN	Vis	0
125	-14.00	-90.00	27.00	-14.22	-90.66	31.40	mVIS	Vis	Vis	0
126	14.00	-87.00	33.00	15.27	-87.09	36.89	mVIS	Vis	Vis	0
127	27.00	-77.00	23.00	28.68	-76.62	25.42	mVIS	DAN	Vis	0
128	19.00	-85.00	-4.00	19.64	-85.62	-2.39	VIS	DAN	Vis	0
129	14.00	-77.00	28.00	15.18	-76.68	31.00	mVIS	Vis	Vis	0
130	-15.00	-53.00	-2.00	-15.85	-52.34	-1.43	mVIS	Vis	Vis	0
131	40.00	-66.00	-8.00	41.60	-65.50	-8.27	DAN	DAN	Vis	0
132	23.00	-87.00	21.00	24.41	-87.21	24.01	mVIS	Vis	Vis	0
133	5.00	-72.00	21.00	5.59	-71.65	23.52	mVIS	Vis	Vis	0
134	-40.00	-73.00	-2.00	-42.10	-73.62	0.38	DAN	DAN	DAN	0
135	25.00	-79.00	-16.00	25.66	-79.47	-15.56	mVIS	DAN	Vis	0
136	-16.00	-77.00	30.00	-16.21	-76.97	33.82	mVIS	Vis	Vis	0
137	-3.00	-81.00	18.00	-2.88	-81.25	21.10	mVIS	Vis	Vis	0
138	-38.00	-87.00	-9.00	-40.21	-88.44	-6.19	DAN	DAN	Vis	0
139	35.00	-84.00	11.00	36.76	-84.11	12.99	mVIS	DAN	Vis	0
140	6.00	-81.00	4.00	6.21	-81.41	6.11	mVIS	Vis	Vis	0
141	-25.00	-89.00	0.00	-26.39	-90.23	3.12	VIS	DAN	Vis	0
142	-31.00	-78.00	-15.00	-33.00	-79.02	-13.24	DAN	DAN	Vis	0
143	35.00	-81.00	0.00	36.51	-81.16	1.20	DAN	DAN	Vis	0

144	-43.00	-2.00	45.00	-43.93	1.80	45.70	CO	SMN	FPC	0
145	45.00	19.00	30.00	47.98	24.56	26.50	aFP	aFPC	FPC	0
146	-45.00	7.00	24.00	-46.50	10.85	23.04	aFP	SMN2	FPC	0
147	-51.00	-50.00	39.00	-52.60	-48.83	42.50	pFP	pFPC	FPC	0
148	56.00	-54.00	-12.00	58.31	-52.79	-13.61	DAN	DAN	FPC	0
149	23.00	39.00	-9.00	24.07	44.61	-15.35	aFP	aFPC	FPC	0
150	32.00	48.00	-6.00	33.60	54.22	-12.95	aFP	aFPC	FPC	0
151	17.00	-79.00	-34.00	16.85	-79.89	-34.36	aDMN	SubCtx	FPC	1
152	34.00	-67.00	-33.00	34.72	-67.08	-34.45	aDMN	SubCtx	FPC	1
153	44.00	5.00	35.00	47.01	9.93	32.66	aFP	aFPC	FPC	0
154	-40.00	2.00	33.00	-41.06	5.81	32.72	aFP	aFPC	FPC	0
155	-41.00	33.00	24.00	-42.23	38.21	21.35	aFP	aFPC	FPC	0
156	36.00	37.00	20.00	38.37	43.18	15.06	aFP	aFPC	FPC	0
157	46.00	-45.00	44.00	49.18	-42.41	45.16	pFP	pFPC	FPC	0
158	-28.00	-59.00	44.00	-28.40	-57.93	47.78	pFP	DAN	FPC	0
159	41.00	-55.00	45.00	43.93	-52.95	46.95	pFP	pFPC	FPC	0
160	35.00	-66.00	38.00	37.45	-64.70	40.38	pFP	pFPC	FPC	0
161	-41.00	-56.00	41.00	-42.09	-54.98	44.74	pFP	pFPC	FPC	0
162	37.00	13.00	42.00	39.87	18.39	39.72	aFP	aDMN	FPC	0
163	-33.00	49.00	9.00	-34.16	54.83	4.36	aFP	aFPC	FPC	0
164	-40.00	40.00	2.00	-41.68	45.16	-2.31	aFP	aFPC	FPC	0
165	31.00	-55.00	42.00	33.38	-53.12	44.02	pFP	DAN	FPC	0
166	41.00	43.00	4.00	43.25	49.25	-2.31	aFP	aFPC	FPC	0
167	-41.00	20.00	31.00	-42.10	24.68	29.53	aFP	aFPC	FPC	0
168	-4.00	21.00	46.00	-2.98	26.41	44.42	aDMN	aDMN	FPC	0
169	9.00	-41.00	48.00	10.51	-38.54	50.02	SM1	SMN	Sal	0
170	52.00	-47.00	36.00	55.27	-44.59	36.70	pFP	pFPC	FPC	0
171	39.00	-5.00	48.00	42.05	-0.39	47.10	CO	SMN	Sal	0
172	29.00	27.00	30.00	31.24	32.79	26.39	aFP	aFPC	Sal	0
173	45.00	17.00	14.00	47.60	22.16	9.74	aFP	aFPC	Sal	0
174	-34.00	16.00	3.00	-35.44	20.03	0.07	CO	CO	Sal	0
175	34.00	17.00	7.00	35.91	21.91	2.62	CO	CO	Sal	0
176	35.00	27.00	3.00	36.89	32.35	-2.24	CO	CO	Sal	0
177	32.00	12.00	-3.00	33.56	16.45	-7.58	aDMN	aDMN	Sal	0
178	-2.00	10.00	45.00	-0.94	14.86	43.99	aDMN	aDMN	Sal	0
179	-27.00	46.00	25.00	-27.50	52.04	21.28	aFP	aFPC	Sal	0
180	4.00	18.00	39.00	5.23	23.22	37.03	aDMN	SMN	Sal	0
181	9.00	17.00	30.00	10.26	22.06	27.48	aDMN	aDMN	Sal	0
182	29.00	49.00	20.00	31.07	55.71	14.49	aFP	aFPC	Sal	0
183	24.00	43.00	31.00	26.07	49.56	26.58	aFP	aFPC	Sal	0
184	-10.00	-21.00	8.00	-10.28	-18.48	7.04	SubC	SubCtx	SubCtx	0
185	11.00	-20.00	9.00	11.75	-17.18	7.54	SubC	SubCtx	SubCtx	0
186	-21.00	4.00	-2.00	-21.97	7.48	-4.78	CO	SubCtx	SubCtx	0
187	29.00	-17.00	4.00	30.50	-13.92	1.65	CO	SubCtx	SubCtx	0
188	22.00	6.00	5.00	23.26	10.19	1.46	CO	SubCtx	SubCtx	0
189	27.00	-3.00	7.00	28.52	0.82	4.01	CO	SubCtx	SubCtx	0
190	-30.00	-14.00	1.00	-31.38	-11.48	-0.30	MotM	SubCtx	SubCtx	0
191	51.00	-45.00	22.00	53.90	-42.76	21.83	tDMN	tDMN	Van	0
192	-54.00	-51.00	8.00	-56.47	-50.48	9.92	tDMN	tDMN	Van	0
193	-53.00	-41.00	12.00	-55.30	-39.89	13.51	tDMN	tDMN	Van	0
194	49.00	-35.00	9.00	51.52	-32.52	7.55	tDMN	tDMN	Van	0
195	49.00	-31.00	-2.00	51.28	-28.52	-4.30	tDMN	tDMN	DMN	0
196	53.00	-48.00	12.00	55.75	-46.07	11.42	tDMN	tDMN	Van	0
197	50.00	27.00	6.00	52.68	32.58	0.57	aFP	Sal	Van	0
198	-47.00	21.00	2.00	-49.07	25.13	-0.98	aFP	Sal	Van	0
199	22.00	-58.00	-22.00	22.43	-57.55	-23.11	mVIS	SubCtx	US	1

200	1.00	-62.00	-18.00	0.51	-61.91	-18.14	SubC	SubCtx	US	1
201	32.00	-15.00	-30.00	32.85	-12.41	-34.41	UNA	DAN	US	0
202	-29.00	-12.00	-33.00	-31.13	-9.99	-36.32	UNA	DAN	US	0
203	47.00	-6.00	-33.00	48.52	-2.85	-38.49	tDMN	tDMN	US	0
204	-47.00	-9.00	-36.00	-50.06	-7.09	-39.24	tDMN	tDMN	US	0
205	8.00	-63.00	57.00	9.61	-61.50	60.88	UNA	SMN	DAN	0
206	-50.00	-63.00	3.00	-52.44	-63.14	5.29	tDMN	DAN	DAN	0
207	-44.00	-51.00	-21.00	-46.68	-50.91	-20.91	DAN	DAN	DAN	0
208	44.00	-48.00	-15.00	45.68	-46.67	-16.85	DAN	DAN	DAN	0
209	44.00	-33.00	48.00	47.21	-29.75	48.70	SM2	SMN2	DAN	0
210	20.00	-66.00	45.00	21.90	-64.74	48.12	pFP	DAN	DAN	0
211	44.00	-60.00	4.00	46.09	-58.93	3.93	DAN	DAN	DAN	0
212	23.00	-60.00	57.00	25.34	-58.18	60.34	SM2	DAN	DAN	0
213	-32.00	-48.00	44.00	-32.56	-46.42	47.20	DAN	DAN	DAN	0
214	-26.00	-71.00	33.00	-26.60	-70.72	36.86	pFP	DAN	FPC	0
215	-32.00	-5.00	53.00	-32.23	-1.08	54.06	CO	SMN	DAN	0
216	-40.00	-60.00	-10.00	-42.26	-60.12	-8.85	DAN	DAN	DAN	0
217	-17.00	-60.00	60.00	-16.50	-58.57	64.46	pFP	DAN	DAN	0
218	26.00	-9.00	54.00	28.56	-4.62	53.99	CO	SMN2	DAN	0
219	48.00	10.00	22.00	50.91	14.99	18.54	aFP	SMN2	FPC	0
220	26.00	4.00	-4.00	27.23	7.96	-8.00	CO	SubCtx	SubCtx	0
221	-8.00	-12.00	58.00	-6.98	-8.08	59.20	SM1	SMN	Mot	0
222	-9.00	10.00	10.00	-9.10	14.14	7.23	aDMN	SubCtx	SubCtx	0
223	-48.00	-66.00	-8.00	-50.61	-66.47	-6.18	DAN	DAN	DAN	0
224	-28.00	42.00	-8.00	-29.34	47.21	-13.27	aFP	aFPC	FPC	0
225	-20.00	2.00	52.00	-19.65	6.39	52.29	aDMN	SMN2	FPC	0
226	20.00	-70.00	-9.00	20.61	-69.94	-8.61	mVIS	Vis	Vis	0
227	12.00	-78.00	38.00	13.31	-77.56	41.66	UNA	Vis	DMN	0
228	56.00	-8.00	-2.00	58.68	-4.28	-5.87	tDMN	tDMN	Van	0
229	39.00	-39.00	-20.00	40.35	-37.36	-22.56	DAN	DAN	DAN	0
230	-20.00	-22.00	64.00	-19.44	-18.61	66.42	SM1	SMN	Mot	0
231	34.00	-84.00	-39.00	34.53	-85.05	-39.74	aDMN	NA	NA	1
232	31.00	-75.00	-54.00	31.06	-75.90	-56.04	CO	NA	NA	1
233	-14.00	-78.00	-24.00	-15.39	-79.00	-23.14	VIS	NA	NA	1
234	-35.00	-51.00	-45.00	-37.82	-51.25	-46.45	aDMN	NA	NA	1

Appendix B. Given the longitudinal nature of our research questions, average FPN and DMN timeseries were computed using ROIs that were reliably assigned to a single network across multiple stages of development (Eggebrecht et al., 2017; Power et al., 2011). Stable FPN ROIs (n = 12) were localized to anterior regions of the brain. Therefore, we also restricted stable DMN ROIs (n = 16) to anterior regions of the brain. As noted in the Methods, new cerebellar ROIs were centered on voxels that exhibited maximal correlations with network average timeseries for the FPN or DMN, with one ROI placed for each hemisphere-network pair (left/right, FPN/DMN). Placement was determined in an independent sample of 24-month children to avoid biasing results. Then, it was visually inspected in our 6-month infant sample to verify that new ROIs captured blood oxygen level dependent (BOLD) signal in every participant. Visual inspection identified 24 ROI observations with insufficient BOLD signal (low-signal ROIs), distributed across 21 subjects (HR+ = 1, HR- = 12, LR- = 8). In univariate analyses, low-signal ROIs were filtered from subject-level datasets using case-wise deletion, and regression coefficients were estimated using maximum likelihood. In multivariate and enrichment analyses, low-signal ROIs were retained to maximize sample size. Functional connectivity values derived from low-signal ROIs (0.2% of data) were normally distributed, with mean and standard deviation (mean = -0.003, sd = 0.038) comparable to high-signal ROIs (mean = 0.013, sd = 0.023).

Appendix C. Spring-embedded graphs (Fruchterman & Reingold, 1992) visualize ROI network affiliations across a range (2%-10%) of edge densities. Cortical ROIs are spherical and cerebellar ROIs are square. Colors denote consensus network assignment (see Figure 2B for legend).

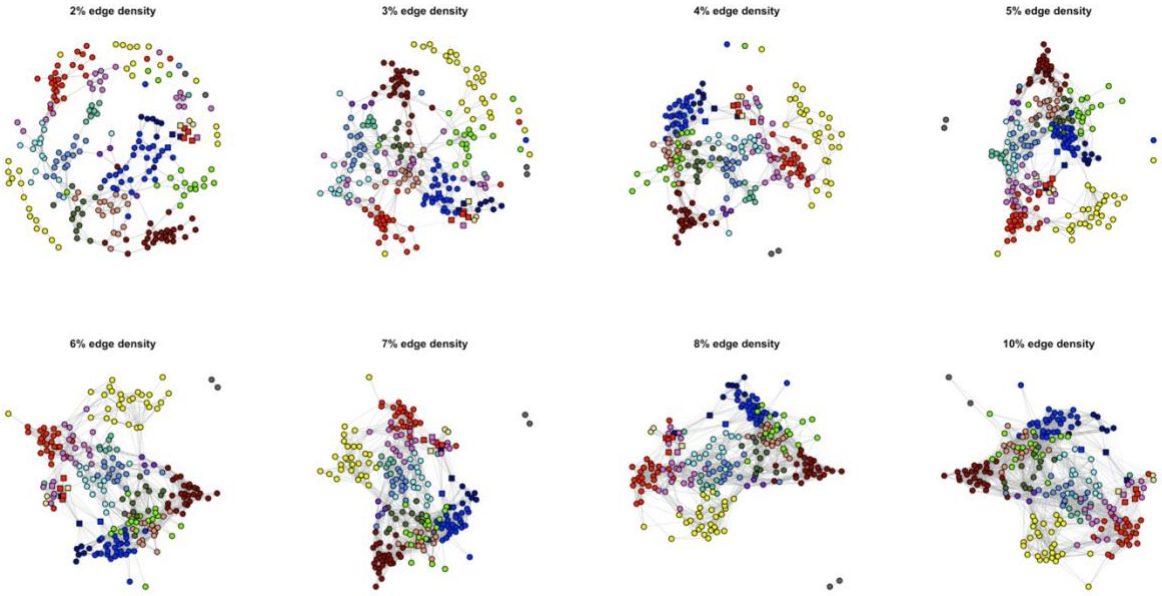

Appendix D. Histograms depict the relationship between adult and infant network assignments for the original set of *n* = 230 ROIs (cf. Eggebrecht et al., 2017). Colors reflect adult network assignments; panels denote infant network assignments.

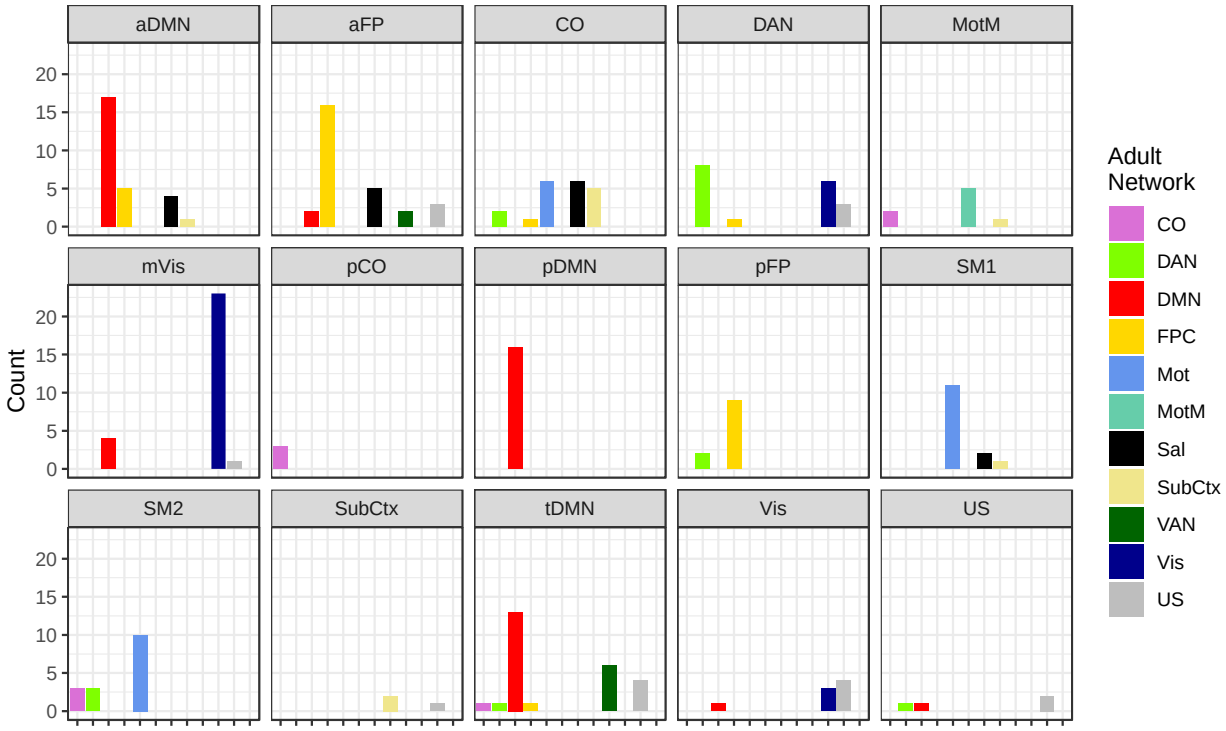

aDMN = anterior default mode network, aFP = anterior frontoparietal network, CO = cingulo-opercular network, DAN = dorsal attention network, MotM = motor-mouth network, mVis = medial visual network, pCO = posterior cingulo-opercular network, pDMN = posterior default mode network, pFP = posterior frontoparietal network, SM1 = somatomotor network 1, SM2 = somatomotor network 2, SubCtx = subcortical network, tDMN = temporal default mode network, Vis = visual network, FPC = frontoparietal control network, Mot = motor, Sal = salience, VAN = ventral attention network, US = unspecified

Appendix E. Secondary validation reinforced the predictive utility of three of four enriched network pairs in relation to later ASD behaviors. Dotted lines indicate the mean error ($\bar{x}E$) in real data, and shaded regions identify randomization runs in which $\bar{x}E_{real} > \bar{x}E_{random}$. (A) Although top principal components derived from functional connections between SM1 and tDMN failed to predict 12-month restricted behaviors ($p = 0.15$), top principal components derived from functional connections between (B) pFP-mVis, (C) aFP-pDMN, and (D) CO-aDMN all predicted the dimensional behaviors from which they were derived (24-month RRBs, 12-month fine motor functioning, and 12-month gross motor functioning, respectively) above chance ($p < .05$).

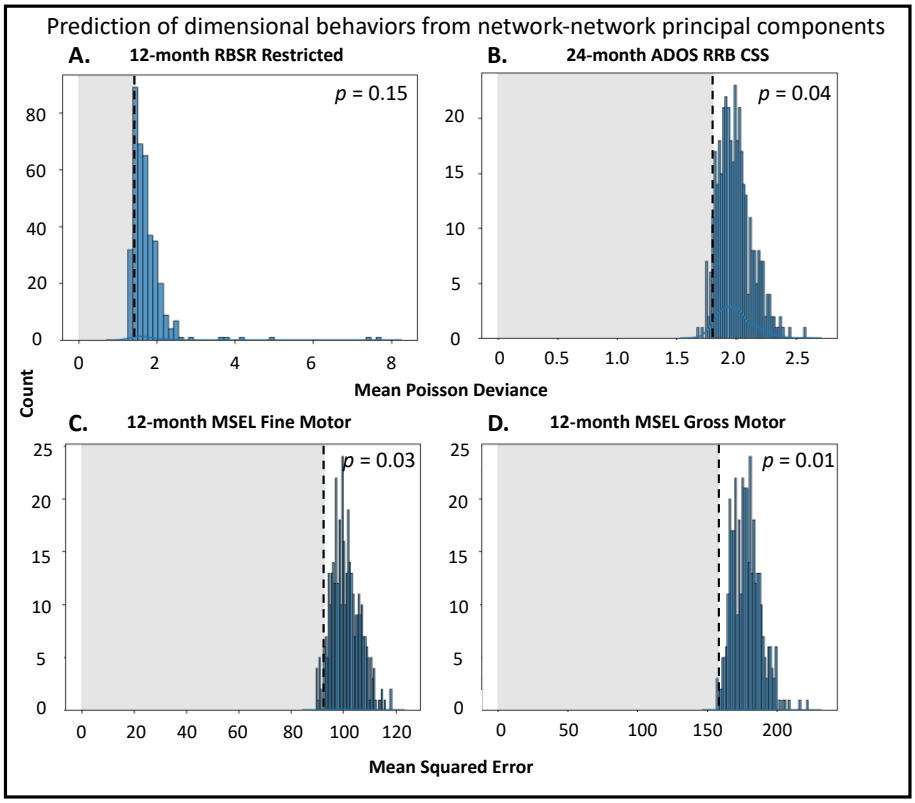

ADOS = Autism Diagnostic Observation Schedule, CSS = calibrated severity score, RRB = restricted interests and repetitive behaviors, RBSR = Repetitive Behavior Scale—Revised, MSEL = Mullen Scales of Early Learning

Appendix F. Cerebellar contributions to network enrichment. Dotted lines indicate the number of cerebellar hits (*n*C) in real data, and shaded regions identify randomization runs in which $nC_{random} > nC_{real}$. (a) Between the cingulo-opercular (CO) and anterior default mode (aDMN) networks, 8.41% of randomization runs included at least as many cerebellar hits as were observed in real data; (b) between posterior frontoparietal (pFP) and medial visual (mVis) networks, 49.17% of randomization runs included at least as many cerebellar hits as were observed in the real data. These results fail to support a statistically significant role for the cerebellum in the emergence of 12- and 24-month ASD behaviors.